JCS ePress online publication date 8 January 2003

Constitutive activation of Rho proteins by CNF-1 influences tight junction structure and epithelial barrier function

Ann M. Hopkins[1,*], Shaun V. Walsh[1], Paul Verkade[2], Patrice Boquet[3] and Asma Nusrat[1]

[1]Epithelial Pathobiology Research Unit, Department of Pathology and Laboratory Medicine, Emory University, Whitehead Biomedical Research Building, Atlanta, GA 30322, USA
[2]Max Planck Institute of Molecular Cell Biology and Genetics, Pfotenhauerstrasse 108, 01307 Dresden, Germany
[3]INSERM Unite 452, IFR 50, Faculté de Medecine, 28 Avenue de Valombrose, F-06107, Nice, France
*Author for correspondence (e-mail: ahopkin@emory.edu)

Accepted 2 December 2002
Journal of Cell Science 116, 725-742 © 2003 The Company of Biologists Ltd
doi:10.1242/jcs.00300

Summary

The apical-most epithelial intercellular junction, referred to as the tight junction (TJ), regulates paracellular solute flux in diverse physiological and pathological states. TJ affiliations with the apical filamentous actin (F-actin) cytoskeleton are crucial in regulating TJ function. F-actin organization is influenced by the Rho GTPase family, which also controls TJ function. To explore the role of Rho GTPases in regulating TJ structure and function, we utilized *Escherichia coli* cytotoxic necrotizing factor-1 (CNF-1) as a tool to activate constitutively Rho, Rac and Cdc42 signaling in T84 polarized intestinal epithelial monolayers. The biological effects of the toxin were polarized to the basolateral membrane, and included profound reductions in TJ gate function, accompanied by displacement of the TJ proteins occludin and zonula occludens-1 (ZO-1), and reorganization of junction adhesion molecule-1 (JAM-1) away from the TJ membrane. Immunogold electron microscopy revealed occludin and caveolin-1 internalization in endosomal-/caveolar-like structures in CNF-treated cells. Immunofluorescence/confocal microscopy suggested that a pool of internalized occludin went to caveolae, early endosomes and recycling endosomes, but not to late endosomes. This provides a novel mechanism potentially allowing occludin to evade a degradative pathway, perhaps allowing efficient recycling back to the TJ membrane. In contrast to the TJ, the characteristic ring structure of proteins in adherens junctions (AJs) was largely preserved despite CNF-1 treatment. CNF-1 also induced displacement of a TJ-associated pool of phosphorylated myosin light chain (p-MLC), which is normally also linked to the F-actin contractile machinery in epithelial cells. The apical perjunctional F-actin ring itself was maintained even after toxin exposure, but there was a striking effacement of microvillous F-actin and its binding protein, villin, from the same plane. However, basal F-actin stress fibers became prominent and cabled following basolateral CNF-1 treatment, and the focal adhesion protein paxillin was tyrosine phosphorylated. This indicates differences in Rho GTPase-mediated control of distinct F-actin pools in polarized cells. Functionally, CNF-1 profoundly impaired TJ/AJ assembly in calcium switch assays. Re-localization of occludin but not E-cadherin along the lateral membrane during junctional reassembly was severely impaired by the toxin. A balance between activity and quiescence of Rho GTPases appears crucial for both the generation and maintenance of optimal epithelial barrier function. Overactivation of Rho, Rac and Cdc42 with CNF-1 seems to mirror key barrier-function disruptions previously reported for inactivation of RhoA.

Key words: Epithelium, Rho GTPases, Tight junction, Paracellular permeability, F-actin

Introduction

Intestinal epithelial cells are physically linked by intercellular junctional complexes that regulate multiple functions, including polarity, mechanical integrity and signaling capacity (Troyanovsky, 1999). The apical-most complex, the tight junction (TJ), regulates barrier function by conferring size selectivity over paracellular transport (Denker and Nigam, 1998; Madara, 1998). TJ proteins include occludin, claudin family members, zonula occludens (ZO) proteins, junction adhesion molecule-1 (JAM-1), along with various scaffolding and signaling molecules. Affiliated with the TJ is a perijunctional filamentous actin (F-actin) ring encircling cells in a 'belt-like' structure, which cooperates with TJ proteins in the regulation of transepithelial permeability or the 'gate function' of epithelial cells, and contributes to permeability regulation (Madara, 1987; Madara et al., 1987; Madara et al., 1988). Contractile events relying on interactions between F-actin and phosphorylated myosin light chain (p-MLC) are especially important in the regulation of nutrient uptake through the sodium-glucose transporter (Turner and Madara, 1995).

The Rho family of small GTPases, comprising Rho, Rac and Cdc42, are critical regulators of F-actin dynamics (Hall, 1998; Nobes and Hall, 1995; Ridley and Hall, 1992). Activation of Rho family members requires guanosine exchange factors

(GEFs), which catalyze the exchange of GDP for GTP. Conformational changes then allow the GTPases to interact with multiple effector molecules involved in actin cytoskeletal control (Aspenstrom, 1999; Hall, 1990). Rho activity cycles are rapidly reversible, and are terminated upon hydrolysis of GTP by GTPase-activating proteins.

The biological consequences of Rho GTPase activation have been extensively explored in mesenchymal cells (Mackay et al., 1997; Nobes and Hall, 1995; Ridley and Hall, 1992; Ridley et al., 1992). How Rho GTPases govern F-actin dynamics in non-mesenchymal cells is less clear. Considering the close apposition between the perijunctional F-actin ring and the epithelial TJ complex, it is conceivable that Rho proteins, through cytoskeletal modification, could affect epithelial barrier function. Several insights have been offered, utilizing diverse pharmacological and molecular tools to interfere with Rho protein function. Our initial investigations utilized a modified cell-permeant chimeric toxin consisting of the *Clostridium botulinum* toxin C3 transferase (to inhibit RhoA activity through ADP-ribosylation of Asp41), and the receptor-binding domain of *Diphtheria* toxin to facilitate internalization (Nusrat et al., 1995). In this system, the barrier function of T84 intestinal epithelial cells was compromised with reductions in transepithelial resistance (TER), enhancements in paracellular permeability and redistribution of ZO-1 and occludin away from the TJ membrane (Nusrat et al., 1995). Related work has focused upon the impact of dominant-active and dominant-negative small GTPase mutants on polarity and barrier function in Madin-Darby canine kidney (MDCK) epithelial cells, and again demonstrated that antagonism of RhoA function can adversely affect TJ structure/function (Jou et al., 1998). Conversely, dominant-active RhoA mutants reportedly protect TJs during ATP depletion (Gopalakrishnan et al., 1998). Mechanisms whereby TJs are influenced by GTPases have recently been reviewed (Hopkins et al., 2000). Our study provides novel insights into the regulation of TJ structure by activated Rho GTPases.

An array of bacterial toxins modulates Rho GTPase function (Aktories, 1997; Boquet, 1999; Boquet et al., 1999; Fiorentini et al., 1998a; Gyles, 1992; Lerm et al., 2000; Schmidt and Aktories, 1998; von Eichel-Streiber et al., 1996). Interference with the cytoskeleton is a common pathogenic mechanism, exemplified by membrane ruffling events or 'cup and pedestal' formation during respectively *Salmonella* and *Escherichia* invasion (Lesser et al., 2000). However, since cytoskeletal rearrangements during *Salmonella* but not *Escherichia* invasion appear under Rho control (Ben-Ami et al., 1998), Rho-independent mechanisms probably exist during distinct forms of bacterial invasion.

Cytotoxic necrotizing factor (CNF-1), a toxin derived from necrotizing *Escherichia coli*, has been implicated in the pathogenesis of prostatitis (Andreu et al., 1997), urinary tract infections (Blanco et al., 1995) and others (Sears and Kaper, 1996). Its mechanism of action involves deamidation of Gln63 of Rho or Gln61 of Rac/Cdc42, resulting in constitutive activation of GTPase signaling via inhibition of GTP hydrolysis (Flatau et al., 1997; Lerm et al., 1999a; Schmidt et al., 1997). CNF-1 was initially identified as a toxin that stimulated the formation of giant multinucleated cells (Caprioli et al., 1983; Caprioli et al., 1984). Bacterial strains secreting CNF-1 are reportedly cytopathic to epithelial cells (De Rycke et al., 1997), however this might reflect the influence of additional virulence factors other than CNF-1 (Island et al., 1998; Island et al., 1999). Evidence actually suggests that CNF-1 protects against apoptosis (Fiorentini et al., 1997; Fiorentini et al., 1998b). Cytoskeletal effects attributed to purified CNF-1 toxin include stimulation of phagocytotic behavior (Falzano et al., 1993), bacterial internalization (Kazmierczak et al., 2001) and stress fiber aggregation in epithelial/mesenchymal cells (Gerhard et al., 1998; Hofman et al., 1998). However, little is known about the effects of CNF-1 on apical F-actin in epithelial cells, including that in the perijunctional ring that is affiliated with TJs. Conflicting reports have suggested both increased (Hasegawa et al., 1999) and decreased (Gerhard et al., 1998) epithelial barrier function following constitutive Rho activation. Our study conducted an in-depth investigation of CNF-1 effects on epithelial TJ structure, barrier function and polarized organization of F-actin/associated proteins. The intestinal epithelial cell line T84 was chosen as a model for our studies (Dharmsathaphorn et al., 1984; Dharmsathaphorn and Madara, 1990; Madara and Dharmsathaphorn, 1985) because its high transepithelial resistance to passive ion flow and well-ordered F-actin/TJ structures make it a stringent model for mechanistic examination of alterations in barrier function. Emphasis was placed on morphological localization of F-actin pools and associated TJ proteins before and after CNF-1 treatment, in an attempt to resolve ambiguities regarding the contribution of Rho proteins to the genesis and maintenance of barrier function in vitro. Our study also presents novel data showing toxin-induced internalization of TJ proteins in caveole and early-/recycling endosomes, suggesting a mechanism for fast re-establishment of barrier function upon CNF-1 removal.

Materials and Methods

Cell culture, CNF-1 incubation and electrophysiology

T84 intestinal epithelial cells were passaged as described (Madara and Dharmsathaphorn, 1985) and seeded on 0.33 or 5 cm^2 collagen-coated permeable supports (Costar, Cambridge, MA). Confluent monolayers were exposed to CNF-1; prepared as described (Falzano et al., 1993) or vehicle (antibiotic-free, serum-free media with 1 mg/ml ultra-pure BSA as carrier protein) for 6-48 hours. TER was measured over time using an epithelial voltohmmeter (EVOM)/EndOhm (World Precision Instruments, Sarasota, FL). On the basis of concentration response curves, 1 nM CNF-1 applied basolaterally was chosen for use in subsequent experiments unless indicated otherwise.

GTPase activation assays

To test for RhoA activation in T84 intestinal epithelial cells upon CNF-1 treatment, a rhotekin-binding assay was performed as previously described (Kranenburg et al., 1999; Sagi et al., 2001; Seasholtz et al., 2001). Briefly, T84 monolayers grown to confluence on 5 cm^2 polycarbonate transwells (Costar) were treated with either CNF-1 (1 nM) or a corresponding volume of vehicle for 24 hours, and harvested into Rho lysis buffer (25 mM HEPES pH 7.4, 125 mM NaCl, 1% Igepal CA-630, 10 mM $MgCl_2$, 1 mM EDTA, 2% glycerol, and protease inhibitors PMSF 250 μM, leupeptin 5 μg/ml, chymostatin 10 μg/ml, pepstatin 0.25 μg/ml, aprotinin 2 μg/ml). Following a brief centrifugation to remove cell debris, lysates from control and CNF-treated cells containing equivalent protein concentrations were rotated for 45 minutes with 40 μL slurry of a GST fusion protein composed of the Rho-binding domain of the specific

Rho effector rhotekin coupled to agarose beads (Upstate Biotechnology, Lake Placid, NY). Addition of GTPγS to additional whole cell lysates served as a positive control for Rho activation. Beads were collected by centrifugation and washed three times with lysis buffer. Beads were resuspended in 2 μL 1M dithiothreitol and 48 μL non-reducing sample buffer, boiled for 5 minutes and subjected to SDS-PAGE on a 12% Tris-HCl gel. Whole cell lysates from both control and CNF-treated cells were run in parallel to determine baseline levels of total RhoA protein. Separated proteins were transferred to nitrocellulose and western blotted with a monoclonal antibody to RhoA (Santa Cruz Biotechnology, Santa Cruz, CA). Using related methods, the activation status of Rac and Cdc42 was also tested in T84 monolayers following CNF-1 treatment. In this case, the Rac effector PAK-1 conjugated to agarose beads was used to pull-down activated Rac from control and CNF-treated monolayers, using a Rac activation assay kit (Upstate Biotechnology). Positive controls consisted of T84 whole cell lysates treated with GTPγS to irreversibly activate Rac. As described above for Rho, activated Rac from the pull-down experiments and total Rac from whole cell lysates was detected by SDS-PAGE and western blot analysis using a monoclonal antibody to Rac.

Since PAK-1 is also an effector for activated Cdc42, the same nitrocellulose membranes were then stripped in β-mercaptoethanol-based buffer and reblotted with a monoclonal antibody to Cdc42 (Upstate Biotechnology).

Paracellular permeability assays

T84 monolayers on permeable supports were exposed apically or basolaterally to CNF-1 or vehicle for 6, 24 or 48 hours. Paracellular permeability to fluorosceinated dextran (FD-3; MW 3000) was assessed according to previously published methods (Sanders et al., 1995). Briefly, TER was measured, monolayers were washed in Hanks balanced salt solution/10 mM HEPES ($HBSS^+$) and then equilibrated at 37°C for 10 minutes on an orbital shaker. Monolayers were loaded apically with 1 mg/ml FD-3 (Molecular Probes, Eugene, OR) at time=zero. Basolateral samples were taken at t=0 and 120 minutes, and fluorescence intensity was analyzed on a CytoFluor 2350 Fluorescence Measurement System (Millipore, Cambridge, MA). FD-3 concentrations transported were extrapolated from a standard curve (generated by diluting known concentrations of fluorescent tracer), and expressed as μM FD-3 transported/cm^2/hour. Numerical values from individual experiments were pooled and expressed as mean ± standard error of the mean (s.e.m.) throughout. Control and test values at each time point of CNF/vehicle treatment were compared by two-tailed unpaired Student's *t*-tests, with statistical significance assumed at P values<0.05.

Immunofluorescence of TJ/adherens junction (AJ) proteins, F-actin and actin-binding proteins

T84 monolayers exposed to CNF-1 or vehicle for 24 hours were washed, fixed in absolute ethanol (20 minutes, –20°C) and blocked in 5% normal goat serum [1 hour, room temperature (RT)]. Monolayers were incubated in humidity chambers for 1 hour with primary antibodies to human occludin, ZO-1, (Zymed Labs, San Francisco, CA), JAM-1 (C. A. Parkos, Emory University, Atlanta, GA), E-cadherin (HECD-1 hybridoma supernatant; A. S. Yap, University of Queensland, Australia), β-catenin, villin, paxillin, caveolin-1, lysosomal-associated membrane protein-1 (LAMP-1; Transduction Laboratories, Lexington, KY), transferrin receptor (Molecular Probes), early endosomal antigen-1 (EEA-1) or Rab11 (Santa Cruz Biotechnology). Monolayers were washed, probed with FITC- or rhodamine-conjugated goat anti-mouse/-rabbit IgG (1 hour, RT; Jackson Immunoresearch Labs, West Grove, PA) and mounted on phosphate-buffered saline/glycerol/*p*-phenylenediamine, 1:1:0.01 (v/v/v). Monolayers double-labeled for p-MLC and ZO-1 were blocked in 3% BSA and co-incubated with goat anti-human p-MLC (Santa Cruz Biotechnology) and rabbit anti-human ZO-1 antibodies. Donkey anti-goat and anti-rabbit antibodies conjugated to fluorescent red or green Alexa dyes (Molecular Probes) were used for detection of the respective primary antibodies. For immunolocalization of filamentous actin (F-actin), monolayers were fixed in 3.7% paraformaldehyde (10 minutes, RT), permeabilized in 0.5% Triton X-100 (30 minutes, RT), incubated with rhodamine-conjugated phalloidin (Molecular Probes; 1 hour, RT), washed and mounted as above. Monolayers were visualized on an LSM510 confocal microscope (Zeiss Microimaging, Thornwood, NY). Images shown are representative of at least six experiments, with multiple images taken per slide.

Immunogold electron microscopy

T84 monolayers treated basolaterally with CNF-1 or vehicle for 24 hours were washed in $HBSS^+$, fixed in 3.7% paraformaldehyde for 20 minutes at room temperature and processed for immunogold electron microscopy as previously described (Nusrat et al., 2000). In short, sections were first labeled with polyclonal antibodies to occludin and detected by protein A coupled to 15 nm gold particles. After fixation and blocking, sections were labeled with polyclonal caveolin-1 antibodies and detected by protein A coupled to 10 nm gold particles. Primary antibodies were omitted from negative control samples. The presence of occludin and caveolin-1 at the TJ was quantitated in control and CNF-1-treated cells. Previously, we had calculated that 90% of the immunogold labeling for occludin was found in the uppermost 250 nm of the basolateral plasma membrane where the apical plasma membranes of two neighboring cells meet (Nusrat et al., 2000). Therefore, numbers of gold particles in this area were counted. Statistical differences between the two occludin groups were tested with a Welch-test since the variances of the two groups were not equal; and statistical differences between the two caveolin-1 groups were tested with a Student's *t*-test.

Immunoblotting for TJ/AJ proteins in epithelial cells

Confluent T84 monolayers on 5 cm^2 permeable supports were incubated basolaterally with CNF-1 or vehicle for 24 hours and washed in $HBSS^+$. Monolayers were scraped into Relax buffer (KCl 100 mM, NaCl 3 mM, $MgCl_2$ 3.5 mM, HEPES pH 7.4 10 mM) containing 1% Triton X-100 with protease inhibitors (as above) and phosphatase inhibitors (sodium fluoride 25 mM, sodium orthovanadate 10 mM). Cell suspensions were dounced 20 times with a Dounce homogenizer, and the nuclei removed by low-speed centrifugation (1500 ***g***, 5 minutes, 4°C). Equivalent concentrations of post-nuclear lysate proteins (10 μg/lane) from control and CNF-treated monolayers were subjected to SDS-PAGE and immunoblotted with antibodies to TJ, AJ and actin-binding proteins (suppliers as above) and actin (Sigma). In order to determine whether CNF-1 caused tyrosine phosphorylation of paxillin, we treated monolayers for 24 hours with CNF-1 or vehicle, prepared lysates and performed SDS-PAGE as above, and immunoblotted with an antibody specific for phospho-paxillin (on Tyr118; Santa Cruz Biotechnology).

Calcium switch assay

T84 monolayers were transiently exposed to ethylene glycol-bis(β-aminoethyl ether)N,N,N′,N′-tetraacetic acid (EGTA; 2 mM, 20 minutes, 37°C) in calcium- and magnesium-free HBSS with 10 mM HEPES ($HBSS^-$) to chelate extracellular calcium and disrupt intercellular junctions (Liu et al., 2000; Parkos et al., 1995). After washing, monolayers were allowed to recover in complete cell culture media (containing calcium) in the presence of CNF-1 or vehicle control. TER was monitored during recovery as an index of TJ function. Additionally, monolayers were fixed and immunostained for

occludin and E-cadherin (as described above) immediately after EGTA treatment, and following 9 hours recovery in the presence of CNF-1 or vehicle.

Results

CNF-1 activates RhoA, Rac and Cdc42 in T84 intestinal epithelial cells

Confluent T84 intestinal epithelial cells were treated with CNF-1 (1 nM, 24 hours) or vehicle, and activation assays performed for Rho, Rac and Cdc42 using agarose-bead-coupled constructs containing the GTPase-binding domain of either the Rho effector rhotekin or the Rac/Cdc42 effector PAK-1. In all cases, the non-hydrolyzable GTP analog GTPγS was used as a positive control for GTPase activation. Total levels of RhoA, Rac and Cdc42 were similar in lysates generated from monolayers treated either with vehicle or CNF-1, or lysates used in positive control experiments (Fig. 1). Greater levels of activated RhoA were pulled down from lysates treated with GTPγS. CNF-1 induced activation of RhoA. In addition, we also observed increased activation of Rac and Cdc42 following incubation of monolayers with CNF-1.

CNF-1 enhances paracellular permeability across intestinal epithelial monolayers

T84 intestinal epithelial cells were grown as polarized monolayers on permeable supports, which at confluence displayed high stable TER to passive ion flow (>1000 Ω.cm^2). As shown in the concentration response curve, basolateral exposure of T84 cells to CNF-1 (0.005-5 nM; plotted on a log scale) for 24 hours evoked significant reductions in TER (Fig. 2). Maximal reductions were observed with 1 and 5 nM CNF-1, hence 1 nM was chosen for subsequent experiments. The bioactive effect of CNF-1 was polarized to the basolateral surface, since apical exposure to toxin did not significantly alter TER over control levels (data not shown).

To complement our electrophysiological observations documenting CNF-induced reductions in TER and to confirm enhanced paracellular permeability, we examined the flux of a macromolecule across T84 monolayers exposed to CNF-1 (Fig. 2; *n*=3-5 experiments). FD-3 was chosen as a marker of paracellular transport (Sanders et al., 1995). T84 epithelial monolayers were treated for 6, 24 or 48 hours with CNF-1 or vehicle, and flux assays performed over the subsequent 2-hour period. Control monolayers (black bars) exposed to vehicle exhibited low levels of FD-3 flux from the apical into the basolateral compartment, which were similar across the three time points measured. FD-3 fluxes across monolayers treated

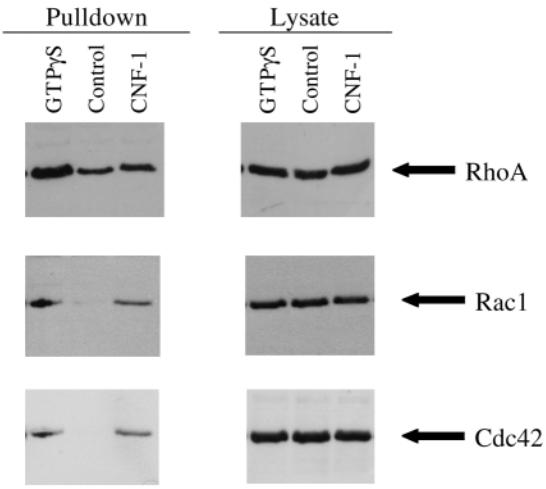

Fig. 1. CNF-1 activates RhoA in T84 intestinal epithelial cells. Confluent T84 intestinal epithelial monolayers were incubated with either CNF-1 (1 nM) or vehicle for 24 hours, and RhoA, Rac1 and Cdc42 activation status was examined by pull-down assays involving binding to the GTPase-binding domains of rhotekin or PAK-1 conjugated to agarose beads. Total Rho, Rac and Cdc42 protein levels were similar in lysates from control and CNF-treated monolayers. However, in pull-down activation assays, more Rho, Rac and Cdc42 were recovered from CNF-treated cells relative to controls, indicating increased activation of these GTPases.

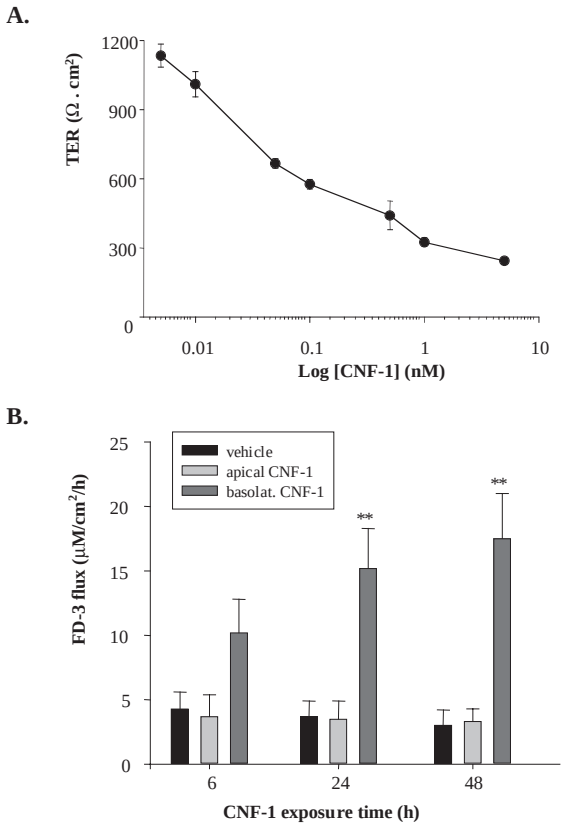

Fig. 2. CNF-1 disrupts TJ gate function in a polarized intestinal epithelial monolayer. T84 monolayers were incubated basolaterally with increasing concentrations of CNF-1 (0.005-5 nM; *n*=4-12 monolayers) for 24 hours. CNF-1 evoked a concentration-dependent reduction in TER that was maximal at ~1 nM (A). In parallel, monolayers were treated either apically (light gray, center) or basolaterally (dark gray) with 1 nM CNF-1 or with vehicle alone (black) for 24 hours (B). Permeation of apically loaded fluorosceinated dextran (FD-3; MW 3000) into the basal compartment over 2 hours was used as an index of passive paracellular transport. Flux of FD-3 across control monolayers and those treated apically with CNF-1 were virtually identical irrespective of CNF-1 incubation time. However, basolateral treatment with CNF-1 augmented FD-3 flux in a time-dependent fashion, which was statistically significant at *t*=24 and 48 hours (*n*≈10 monolayers per condition).

apically with CNF-1 (light gray bars) were statistically indistinguishable from controls at the same time points. However, monolayers treated basolaterally with CNF-1 (dark gray bars) showed significant enhancements in paracellular flux of FD-3. Permeability enhancements were dependent upon the length of exposure to the toxin, with flux following 24 or 48 hours incubation with CNF-1 being significantly different to control fluxes at the same time points ($P<0.01$).

CNF-1 induces redistribution of key TJ proteins involved in epithelial barrier function

Since the epithelial TJ protein complex is a major regulator of transport through the paracellular route, we examined the effect of CNF-1 on the immunolocalization of candidate TJ proteins (Fig. 3). T84 intestinal epithelial monolayers incubated either apically or basolaterally with CNF-1 (1 nM, 24 hours) or vehicle control were immunostained with antibodies to occludin, ZO-1 and JAM and examined by confocal microscopy. Occludin distribution in control T84 epithelial monolayers (Fig. 3a) mirrored that in monolayers incubated apically with CNF-1 (Fig. 3b); namely a characteristic cobblestone pattern shown in en face confocal micrographs captured at the level of the TJ. Monolayers incubated basolaterally with CNF-1 (Fig. 3c) displayed occludin reorganization in the TJ plane, manifested as decreased occludin localization at the TJ membrane (arrow) with potential internalization (#). Total occludin protein levels (Fig. 3j) were similar in cell lysates from both control (lane 1) and CNF-treated monolayers (lane 2).

The morphological distribution of another TJ protein, ZO-1, a cytoplasmic plaque protein that affiliates with the underlying

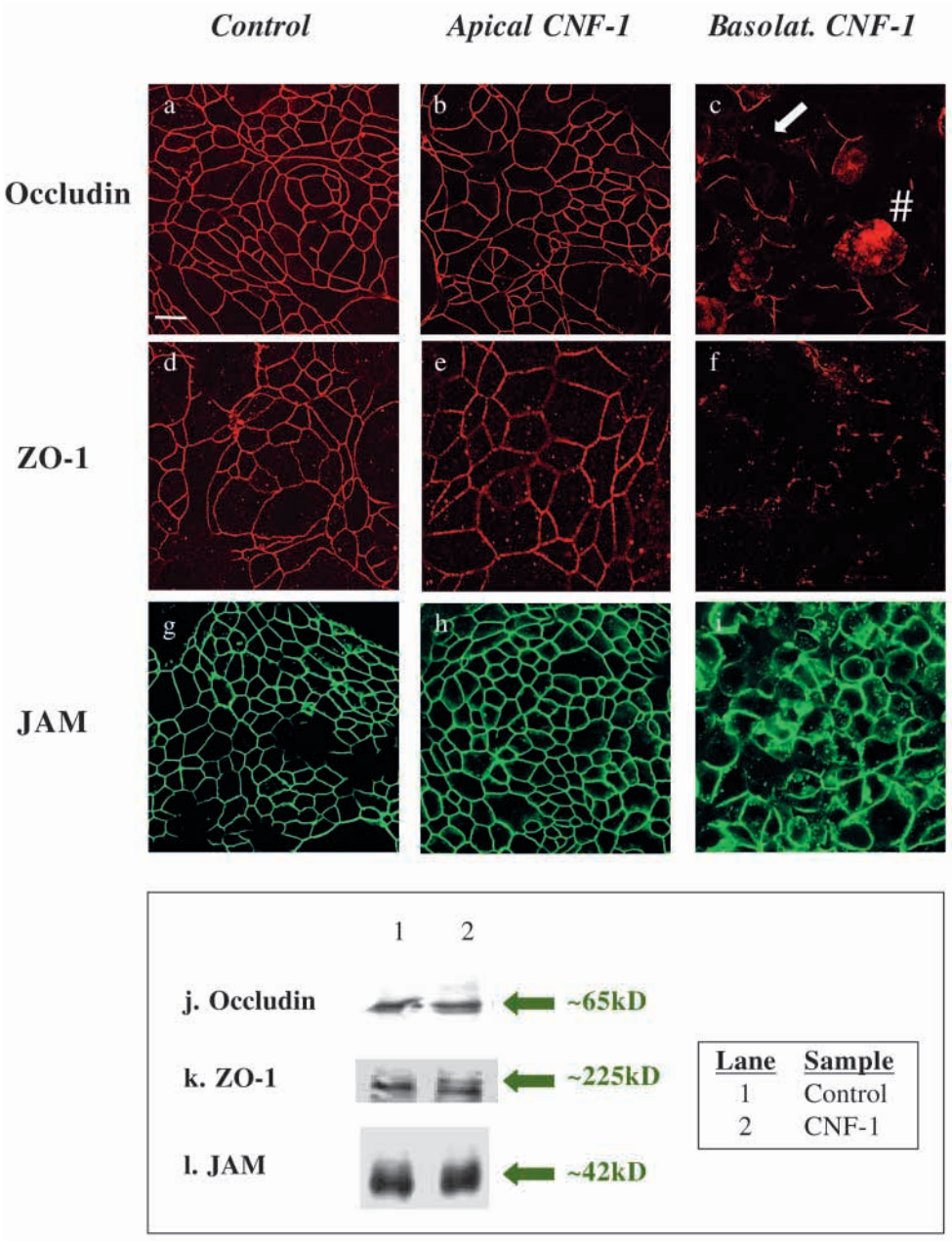

Fig. 3. CNF-1 alters morphological localization of candidate TJ proteins. T84 monolayers were exposed to CNF-1 or vehicle alone for 24 hours, and TJ proteins occludin, ZO-1 and JAM were localized by immunofluorescence and confocal microscopy. In control monolayers (a), occludin localized sharply in the apical region of the lateral membrane, visualized en face as a ring pattern. Monolayers treated apically for 24 hours with CNF-1 (b) were identical. Monolayers exposed basolaterally to CNF-1 for 24 hours (c) displayed dramatic redistribution of occludin away from the lateral TJ membrane (arrow). ZO-1 staining in control monolayers (d) resembled that of occludin, outlining TJs just below the apical plane. Apical exposure to CNF-1 for 24 hours did not affect ZO-1 immunolocalization (e); however, discontinuities in ZO-1 ring structures were evident in monolayers treated basolaterally with CNF-1 for the same time period (f). JAM in control monolayers (g) was enriched in the TJ plane, and unchanged by apical treatment with CNF-1 toxin for 24 hours (h). However, basolateral exposure to CNF-1 for the same time period (i) somewhat disrupted JAM distribution, with diffusion away from the TJ membrane into the cytoplasm. Levels of occludin (j), ZO-1 (k) or JAM (l) proteins were minimally different in lysates prepared from control (lane 1) versus CNF-treated (lane 2) epithelial monolayers. Bar≈10 μm.

F-actin cytoskeleton, was also examined. ZO-1 staining in control monolayers (exposed to vehicle alone; Fig. 3d) resembled that of occludin, being confined to distinctive TJ ring formations. No substantial alterations were visible upon apical exposure to CNF-1 toxin (Fig. 3e); however basolateral exposure to toxin for the same time period (Fig. 3f) stimulated dramatic reorganization of ZO-1 away from the TJ plane. Like occludin in cells treated basolaterally with CNF-1, there was partial or, in some cases, complete loss of the ring structure that is morphologically characteristic of these proteins in en face confocal images. All images presented are representative of at least four independent experiments, and all morphological alterations were similar or intensified upon prolonged basolateral incubation with CNF-1 (48 hours). Morphological reorganization events were not accompanied by alterations in the total ZO-1 protein levels in control versus CNF-treated monolayers (Fig. 3k).

The ring pattern of JAM-1 immunolocalization in en face images of control monolayers (Fig. 3g) resembled that of occludin and ZO-1, with sharp rings indicative of localization at the distinct lateral TJ membrane. Some additional staining was observed along the lateral membrane in the *xz* or vertical plane (not shown). JAM distribution in TJs of monolayers treated apically with CNF-1 for 24 hours (Fig. 3h) was virtually identical to that in control monolayers. By contrast, monolayers exposed basolaterally to CNF-1 for 24 hours (Fig. 3i) displayed some loss of JAM definition at the membrane. The 'blurred' rings probably represent some JAM redistribution away from the TJ membrane to a cytoplasmic region just below the lateral membrane. This could be important in the loss of barrier function since the presence of JAM at the TJ membrane is essential for correct re-localization of occludin during TJ assembly (Liu et al., 2000). Western blot data (Fig. 3l) did not reveal any differences in total JAM protein levels between control and CNF-treated monolayers.

CNF-1 induces internalization of occludin and caveolin-1 in caveolar/recycling endosomal structures

By immunogold electron microscopy, we have previously shown that occludin predominantly (>90%) localizes to the apical-most 250 nm of the basolateral plasma membrane (Nusrat et al., 2000). In control epithelial cells, occludin (pseudo-colored in red) displays this pattern (Fig. 4Aa, arrow); however, upon basolateral treatment of the cells with CNF-1 for 24 hours, some occludin disappeared from this TJ domain into an intracellular compartment (Fig. 4Ab, #). A percentage of internalized occludin moved into membranous structures ultrastructurally resembling endosomes/caveolae (Fig. 4Ac), and co-localized with caveolin-1, a caveolar scaffolding protein (particles colored in black). We quantitated the redistribution of occludin and caveolin-1 from TJs after CNF-1 treatment (Fig. 4B, occludin in n=25 TJs; caveolin-1 in n=10 TJs for both control and CNF-treated cells). In control cells, we found 6.8±0.5 occludin gold particles per TJ (mean±s.e.m.) while, in CNF-treated cells, we only found 1.9±0.3 occludin gold particles per TJ domain. This approximately 3.5-fold difference was statistically significant (P<0.00001). Analogous to our findings with occludin, caveolin-1 was also re-distributed away from the TJ following CNF-1 incubation. We observed 6.7±0.6 caveolin-1 gold particles per TJ in control cells, but only 2.4±0.4 caveolin-1 gold particles (P<0.0001) per TJ of CNF-treated cells. Similar trends were seen for ZO-1 internalization (data not shown).

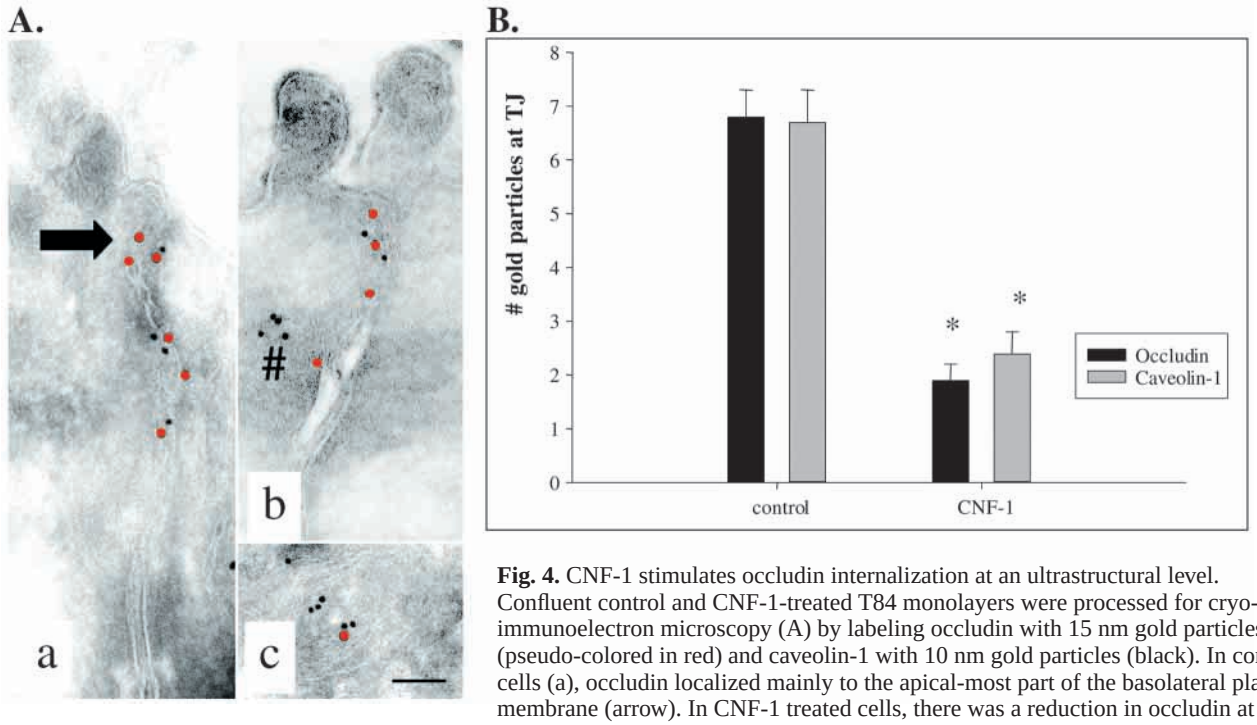

Fig. 4. CNF-1 stimulates occludin internalization at an ultrastructural level. Confluent control and CNF-1-treated T84 monolayers were processed for cryo-immunoelectron microscopy (A) by labeling occludin with 15 nm gold particles (pseudo-colored in red) and caveolin-1 with 10 nm gold particles (black). In control cells (a), occludin localized mainly to the apical-most part of the basolateral plasma membrane (arrow). In CNF-1 treated cells, there was a reduction in occludin at the plasma membrane of the TJ domain (b, #). Some labeling was now found to co-localize with caveolin-1 in intracellular caveolae and endosomal-like compartments (c). Bar, 100 nm. Following quantitation of occludin (black bars) and caveolin-1 (gray bars) gold particles at the TJ, statistically significant reductions in both proteins were observed in CNF-treated monolayers relative to controls (B).

In order to address more precisely the nature of the structures into which occludin was internalized upon CNF-1 treatment (1 nM, 24 hours), we performed double-immunolabeling/confocal microscopy for occludin and a range of endosomal/caveolar markers. Occludin in control cells co-localized with a TJ-associated pool of caveolin-1 (Fig. 5a2, arrowhead) in ring structures distinct from the large pool of caveolin-1 highlighting the apical brush border. Upon treatment with CNF-1, internalization of occludin (Fig. 5b1, arrows) and caveolin-1 (Fig. 5b2, arrowheads) was observed. Areas of co-localization between internalized occludin and caveolin-1 are shown in Fig. 5b3 (#). Occludin staining following CNF-1 incubation was also examined in the context of the early endosomal markers EEA-1 and the transferrin receptor. The transferrin receptor exhibited diffuse cytoplasmic staining in control cells (Fig. 5c2), and no overlap with occludin (Fig. 5c3) was observed. Following CNF-1 incubation and characteristic occludin internalization (Fig. 5d1, arrow), the transferrin receptor was observed to condense into areas also suggestive of internalization sites (Fig. 5d2, arrowhead). However, although neighbors, these internalization sites seemed morphologically distinct from each other (Fig. 5d3, #). EEA-1 in control cells (Fig. 5e2) displayed a diffuse cytoplasmic staining pattern similar to that of the transferrin receptor, in addition to a distinct membranous pool in rings (Fig. 5e2, arrow) that co-localized with those of occludin (Fig. 5e1, occludin alone; Fig. 5e3, composite of occludin and EEA-1). Internalization of occludin induced by exposure to CNF-1 (Fig. 5f1, arrows) occurred in compartments similar to those of internalized EEA-1 (Fig. 5f2, arrowheads). Morphological overlap of some of these internalized structures (Fig. 5f3, #) suggests that at least a pool of occludin can be internalized in EEA-1-positive early endosomes following CNF-1 treatment.

We next explored the possibility that this sub-pool of early endosomes could be recycling endosomes, which target their cargo back to the membrane rather than onwards to late endosomes/lysosomes (Casanova et al., 1999; Ullrich et al., 1996). Thus, we stained for occludin and the recycling endosomal marker Rab11 in control cells and those treated with CNF-1. Rab11 positivity in control cells (Fig. 5g2) seemed to be confined to sub-membranous structures resembling vesicles. No co-localization with the characteristic TJ rings of occludin was observed in control cells (Fig. 5g1, occludin alone; Fig. 5g3, occludin/Rab11 composite). However, following treatment with CNF-1, internalization of occludin (Fig. 5h1, arrow) and condensations of Rab11 (Fig. 5h2, arrowhead) partially overlapped with each other (Fig. 5h3, #). This suggests that at least a pool of internalized occludin might be recycled back to the membrane in Rab11-positive recycling endosomes.

Since our biochemical experiments showed that occludin was not degraded following CNF-1 treatment, we double-stained monolayers for occludin and the late endosomal marker LAMP-1. Anti-LAMP-1 stained control T84 cells (Fig. 5i2) in a characteristic ring pattern reminiscent of, but not coincident with, occludin (Fig. 5i1). In the composite image (Fig. 5i3), it can be seen that both these proteins are in the same plane but are mainly adjacent to each other rather than in an overlapping pattern (#). Incubation with CNF-1 induced fragmentation of LAMP-1 rings, with apparent internalization in sub-membranous vesicles (Fig. 5j2). Absolutely no overlap was observed between areas of internalized occludin (Fig. 5j1, arrows; Fig. 5j3, #) and LAMP-1 positivity, suggesting that occludin internalized after CNF-1 treatment is not designated for a lysosomal degradative pathway. In addition, there was a lack of co-localization between internalized occludin and clathrin following incubation with CNF-1 in our system (data not shown).

CNF-1 does not abolish the localization of AJ proteins in ring structures at cell-cell borders

Immunolocalization of E-cadherin and β-catenin was performed in order to evaluate the influence of CNF-1 on AJs. As shown in Fig. 6, in control cells both E-cadherin (Fig. 6a) and β-catenin (Fig. 6c) were visualized in a ring pattern by en face confocal imaging, consistent with their localization in AJs. Minor changes in both E-cadherin (Fig. 6b) and β-catenin (Fig. 6d) distribution were observed following basolateral incubation with CNF-1 for 48 hours, mainly a slight increase in staining intensity at cell-cell borders, or potentially a subtle diffusion of the same away from the membrane. However, the localization of both E-cadherin and β-catenin in ring structures was essentially preserved despite CNF-1 treatment, in contrast to ring structures of TJ proteins that were severely disrupted under the same conditions. Expression of total cellular E-cadherin and β-catenin was not influenced by CNF-1 treatment for various time periods, as determined by western blot analysis (Fig. 6e,f respectively; lanes 1-3 control, lanes 4-6 CNF-1).

CNF-1 alters the localization of a TJ-associated pool of p-MLC

TJ proteins affiliate with the underlying perijunctional F-actin ring and this affiliation is important in the regulation of TJ function (Madara, 1987). In addition, MLC phosphorylation has also been shown to regulate TJ function (Turner and Madara, 1995). Therefore, we investigated whether epithelial exposure to CNF-1 could alter the distribution of p-MLC in TJs. There was extensive co-localization between the ring structures of ZO-1 and a pool of p-MLC at the level of the TJ in control T84 epithelial cells (Fig. 7a-c). This co-localization was mirrored in monolayers treated apically for 24 hours with CNF-1 (Fig. 7d-f). However, upon basolateral treatment with the toxin, severe disruption in the perijunctional staining pattern of not only ZO-1 (Fig. 7g) but also p-MLC (Fig. 7h) occurred. Almost complete fragmentation of the ring structures of both proteins was observed at the level of the TJ, although punctate fragments of ZO-1 and p-MLC that remained in the TJ plane still exhibited some co-localization (Fig. 7i).

CNF-1 induces polarized reorganization of F-actin and select actin-binding proteins

Since TJs have previously been shown to affiliate with F-actin (Madara, 1987; Madara et al., 1987; Madara et al., 1988), and since actin-myosin contraction is an important regulator of paracellular permeability (Turner and Madara, 1995), we examined in detail the effects of CNF-1 treatment on the organization of polarized pools of F-actin and associated binding proteins in epithelial cells. F-actin architecture in T84

monolayers was highlighted by rhodamine-phalloidin staining and confocal microscopy following 6 hours exposure to either CNF-1 (1 nM) or vehicle (Fig. 8a-l). Fig. 8a represents en face imaging at the level of the apical membrane. F-actin in this plane is organized in characteristic perijunctional rings (arrowhead) and, in the apical brush border, as fine dot-like staining representing microvillous actin cores (*). This pattern was unaltered following apical incubation with CNF-1 toxin

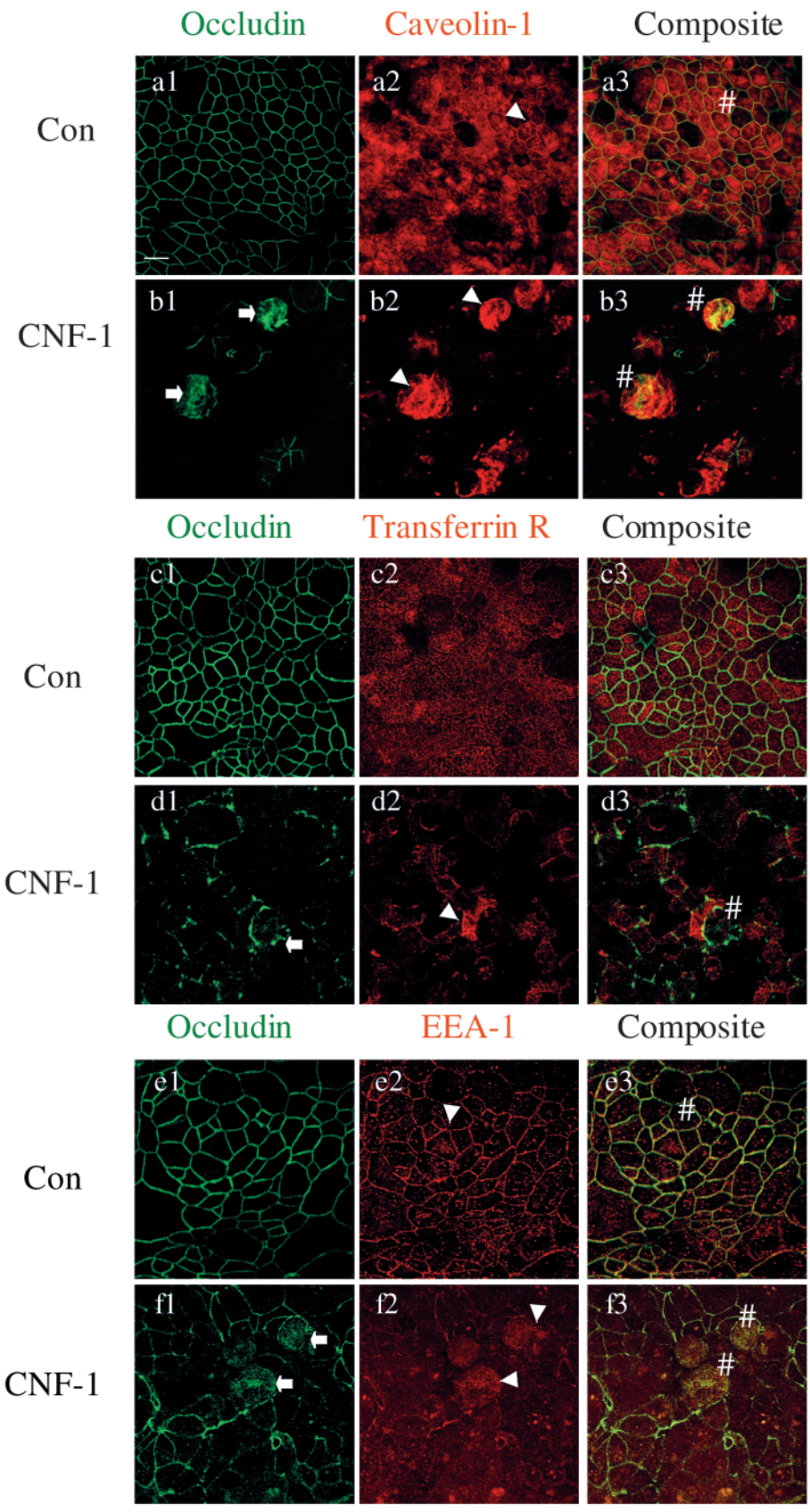

Fig. 5. CNF-induced internalization of occludin is via caveolae and early-/recycling endosomes but not late endosomes. T84 epithelial monolayers were incubated with vehicle or CNF-1 (1 nM) for 24 hours, and the internalization of occludin monitored in relation to markers of endosomal/caveolar pathways by immunofluorescence/confocal microscopy. Occludin in the en face plane of control cells (a1, c1, e1, g1, i1) was characteristically distributed in discrete TJ rings at cell-cell borders. Caveolin-1 staining in control cells (a2) consisted of a large pool of apical staining, together with a sub-pool of caveolin-1 localizing in a ring pattern at TJs (arrowhead). This was observed to co-localize with occludin (a3, #). Occludin internalization in CNF-treated cells (b1, arrows) was seen to correspond closely with a pool of internalized caveolin-1 in the same cells (b2, arrowheads) and in a composite image (B3, #). The transferrin receptor in control cells (c2) localized mainly to the apical surface and underneath the membrane, showing no overlap (c3) with the staining pattern for occludin. Following CNF-1 incubation, internalized occludin (d1, arrow) and internalized transferrin receptor (d2, arrowhead) did not appear to co-localize with each other (d3, #). Another early endosomal marker, EEA-1, localized to sub-membranous structures with some additional staining at the TJ membrane (E2, arrowhead). This, like caveolin-1 staining in control cells, overlapped with occludin (e3, #). Occludin internalization upon CNF-1 incubation (F1, arrows) overlapped with EEA-1 distribution in the same cells (F2, arrowheads). This overlap in the merged image (f3, #) suggests internalization of occludin in EEA-1-positive early endosomes. Distribution of the recycling endosomal marker Rab11 was primarily sub-membranous in control cells (g2), showing no co-localization with occludin (g3). However, occludin (h1, arrow) and Rab11 (h2, arrowhead) internalization in CNF-treated monolayers were observed to overlap significantly (h3, #). The late endosomal marker LAMP-1 localized to the membrane at the level of intercellular junctions in control cells (i2), in a pattern that resembled but did not overlap with (i3, #) that of occludin. Occludin internalization after CNF-1 treatment (j1) did not co-localize with LAMP-1-positive late endosomes in the same cells (j3, #). Results are representative of ~6 experiments. Bar≈10 μm.

(Fig. 8b). While perijunctional F-actin ring staining was preserved (or perhaps even enhanced) in response to basolateral treatment with CNF-1 (Fig. 8c), a striking abolition of microvillous actin staining was observed (arrow). This was complemented by alterations in the staining patterns of villin, a major actin-regulating protein enriched in apical epithelial brush borders. In control monolayers (Fig. 8d) and those treated apically with CNF-1 (Fig. 8e), en face images revealed identical villin staining patterns in F-actin-rich microvillous cores. Villin staining intensity in the apical plane was significantly diminished following basolateral treatment with CNF-1 (Fig. 8f), suggesting brush border effacement.

At the basal pole of both control (Fig. 8g) and apically treated (Fig. 8h) monolayers, F-actin stress fibers were observed as a meshwork of filaments. In contrast to the effacement of brush border F-actin, basolateral exposure to CNF-1 (Fig. 8i) induced aggregation of stress fibers into prominent bundles with a 'cabled' appearance. Enhancements in both stress fiber number and aggregation have been previously observed in non-polarized cells such as fibroblasts transfected with dominant active RhoA (Ridley and Hall, 1992). This is a hallmark feature confirming the specific activation of RhoA. Since stress fiber changes were observed following CNF-1 incubation, we also examined the distribution of an actin-binding protein in the same region of the cells. In control monolayers, the actin-binding protein paxillin was seen as small plaques consistent with its distribution in focal cell-matrix contacts (Fig. 8j). Monolayers treated apically with CNF-1 displayed a similar staining pattern for paxillin (Fig. 8k). However, basolateral incubation with CNF-1 (Fig. 8l) induced a small increase in paxillin plaques. All morphological alterations in F-actin/actin-binding proteins induced by CNF-1 occurred independently of biochemical alterations in protein levels at all sampled time points, as shown by western blot data (Fig. 8m-o). Actin levels in control (Fig. 8m, lanes 1-3) versus CNF-treated (lanes 4-6) lysates appeared similar, as did villin levels under the same conditions (Fig. 8n, lanes 1-3 control, lanes 4-6 CNF-1). A slight increase in the molecular mass of paxillin was noticed in lysates from CNF-treated monolayers at all time points shown (Fig. 8o, lanes 1-3 control, lanes 4-6 CNF-1). When lysates from control and CNF-treated (1 nM, 24 hours) monolayers were blotted with an antibody specific for tyrosine-phosphorylated paxillin (Fig. 8p), a substantial increase in phospho-paxillin was detected in CNF-treated samples. We also observed increased tyrosine phosphorylation of paxillin in CNF-treated cells following immunoprecipitation with anti-paxillin and immunoblotting with anti-phospho-paxillin (data not shown). Tyrosine phosphorylation of paxillin has previously been observed in other systems following Rho GTPase activation (Imamura et al., 2000; Sinnett-Smith et al., 2001).

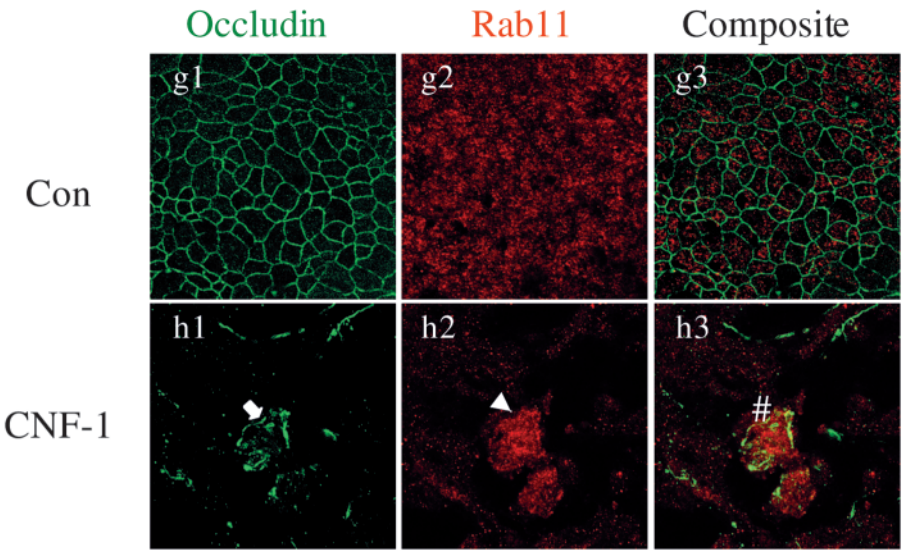

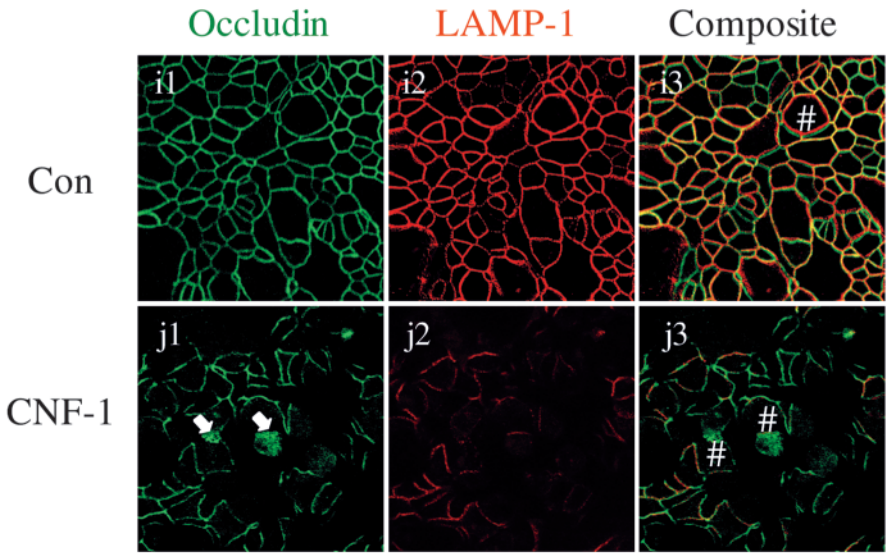

CNF-1 impairs intercellular junction assembly

Transient depletion of extracellular calcium is a well-validated model for studying the assembly of intercellular junctional contacts. Since CNF-1 influenced TJs in stable polarized epithelial cells, we examined the influence of Rho GTPase activation by CNF-1 on assembly of intercellular contacts and recovery of barrier function. As shown (Fig. 9A), the baseline TER of monolayers subsequently incubated with vehicle (closed circles) or CNF-1 (open circles) were similarly high before calcium depletion (#). Following EGTA treatment, TER predictably dropped to below 100 $\Omega.cm^2$, whereupon

monolayers were washed and allowed to recover in calcium-containing media in the presence or absence of CNF-1 (1 nM). Control monolayers recovered high TER values of ~700 $\Omega.cm^2$ by 6 hours following repletion of extracellular calcium. This corresponds to the presence of assembled TJs in the monolayer (Liu et al., 2000). By contrast, monolayers exposed to CNF-1 during the recovery period failed to recover TER (162±14 $\Omega.cm^2$ 24 hours after EGTA washout and calcium repletion). To answer the question of whether this related to inhibitory effects of CNF-1 on nascent AJs as well as TJs, we examined E-cadherin and occludin distribution in monolayers after EGTA treatment and during recovery in the presence of CNF-1 or vehicle. Following EGTA treatment (Fig. 9B), both occludin (a) and E-cadherin (b) were localized intracellularly rather than at their respective junctions. Redistribution of both these proteins back to the lateral membrane was evident in control cells 9 hours later (c,d). However, occludin did not correctly redistribute back to the membrane in monolayers exposed to CNF-1 during recovery (e). It was instead observed in punctate dots that may mark tricellular corners. E-cadherin movement back to the membrane in CNF-treated cells (f) resembled that in control cells, further indicating preferential disruption of the TJ over the AJ by CNF-1. These findings illustrate that overactivation of Rho GTPases impairs not only the barrier function of mature TJs, but is also detrimental for the assembly of nascent TJs and the acquisition of barrier properties.

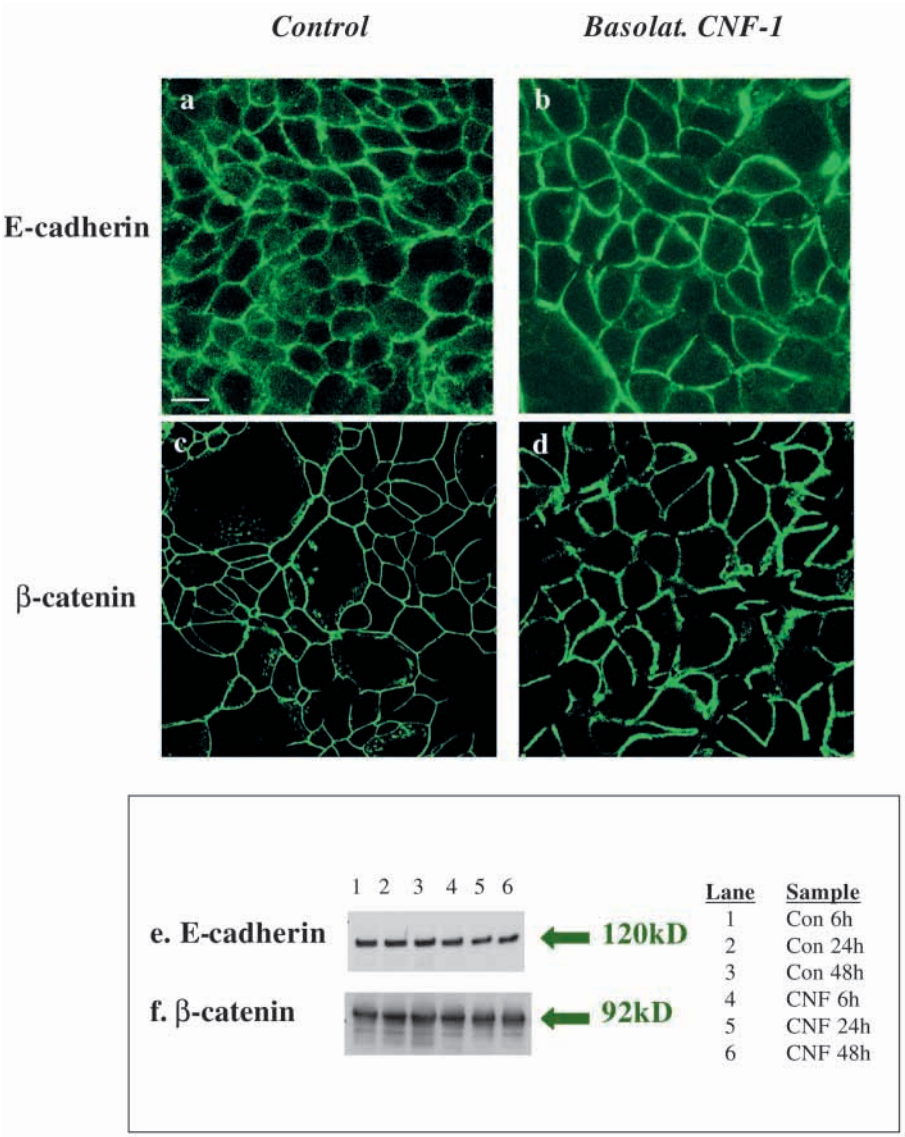

Fig. 6. CNF-1 does not dramatically influence AJ protein localization in the lateral membrane. E-cadherin and β-catenin were immunolocalized in confluent T84 monolayers exposed basolaterally to CNF-1 (1 nM, 48 hours) or vehicle. In control monolayers, both E-cadherin (a) and β-catenin (c) were visualized en face in characteristic ring formations in the AJ. Basolateral exposure to CNF-1 did not visibly alter the ring pattern of E-cadherin (b), although minor thickening of β-catenin staining intensity was observed at cell-cell borders (d). Total protein levels of E-cadherin (e) and β-catenin (f) were unaffected by CNF-1 treatment (lanes 1-3 control, 4-6 CNF-1). Bar≈10 μm.

Discussion

Since studies have revealed a role for Rho GTPases in regulating TJ structure/function (Nusrat et al., 1995; Jou and Nelson, 1998; Jou et al., 1998), we further explored the mechanisms whereby paracellular permeability is influenced by this family of mediators. CNF-1 was used as a tool to activate consitutively Rho GTPases by deamidation of Gln61/63 (Flatau et al., 1997; Schmidt et al., 1997). We observed activation of RhoA, Rac1 and Cdc42 following incubation of polarized T84 intestinal cells with CNF-1, as confirmed by pull-down assays utilizing binding to the specific Rho effector rhotekin or the Rac/Cdc42 effector PAK-1 (Kranenburg et al., 1999; Sagi et al., 2001; Seasholtz et al., 2001). Interestingly, levels of activated Rac and Cdc42 detected in these assays exceeded those of activated RhoA. This might relate to several factors. First, GTPase-activating proteins selective for Rho (Rho-GAPs) might be highly active, resulting in a loss of Rho-GTP signal. Second, since caveolae close to the cell surface are enriched in Rho that is either pre-activated or ready to be activated (Michaely et al., 1999), it is likely that even small changes in levels of activated RhoA in that specialized microenvionment are highly significant. Since TJs also exist in lipid-raft-associated membrane microdomains (Nusrat et al., 2000), high local levels of activated Rho could have important functional consequences for the structure and function of TJ proteins.

The functional consequences of Rho, Rac and Cdc42 activation by CNF-1 in our model included the induction of parallel reductions in TER and enhancements in paracellular permeability. This response was polarized to basolateral incubation with CNF-1. The C terminus of CNF reportedly harbors the cell-binding domain

(Lemichez et al., 1997), mediating clathrin-independent endocytosis requiring transient membrane acidification (Contamin et al., 2000).

Reported effects of the activation of Rho GTPases by CNF-1 on epithelial TER have to date been ambiguous. Interference with signaling could cause: (1) increased TER; (2) decreased TER; or (3) no change in TER. One report suggests that CNF-1 does not affect TER (Hofman et al., 1998), however our results support observations of CNF-induced reductions in TER in another well-polarized epithelial cell line, Caco-2 (Gerhard et al., 1998). Since CNF-1 simultaneously activates Rho, Rac and Cdc42, it is difficult in this model to dissect out the specific contributions of individual GTPases to observed changes in barrier function. However, some information can be gained by using specific pharmacological inhibitors of the RhoA pathway in combination with CNF-1. We used the RhoA inhibitor C3 toxin to examine whether inhibition of RhoA in T84 cells could protect against the barrier-disruptive effects of CNF-1 (data not shown). Pre-incubation of the cells with low concentrations of C3 caused a reproducible drop in TER, which was not prevented by application of CNF-1 (data not shown). Similarly, simultaneous incubation of cells with CNF-1 and C3 evoked profound disruptions in TER (data not shown). We also tried to block the effects of CNF-1 on epithelial TER using the Rho kinase inhibitor Y-27632. However, since this by itself also compromises epithelial barrier function (Walsh et al., 2001), we did not observe any protective effect against the influence of CNF-1 (data not shown). Thus, in our model, the effects of CNF-1 were not blocked by inhibitors of RhoA or Rho kinase, verifying that RhoA is not the sole factor responsible for reductions in TER and barrier function. Given that all compounds (CNF-1, C3, Y-27632) adversely affect the barrier function of epithelial cells, this supports the notion that a delicate balance of Rho activity/quiescence must be maintained in order to preserve optimal barrier function.

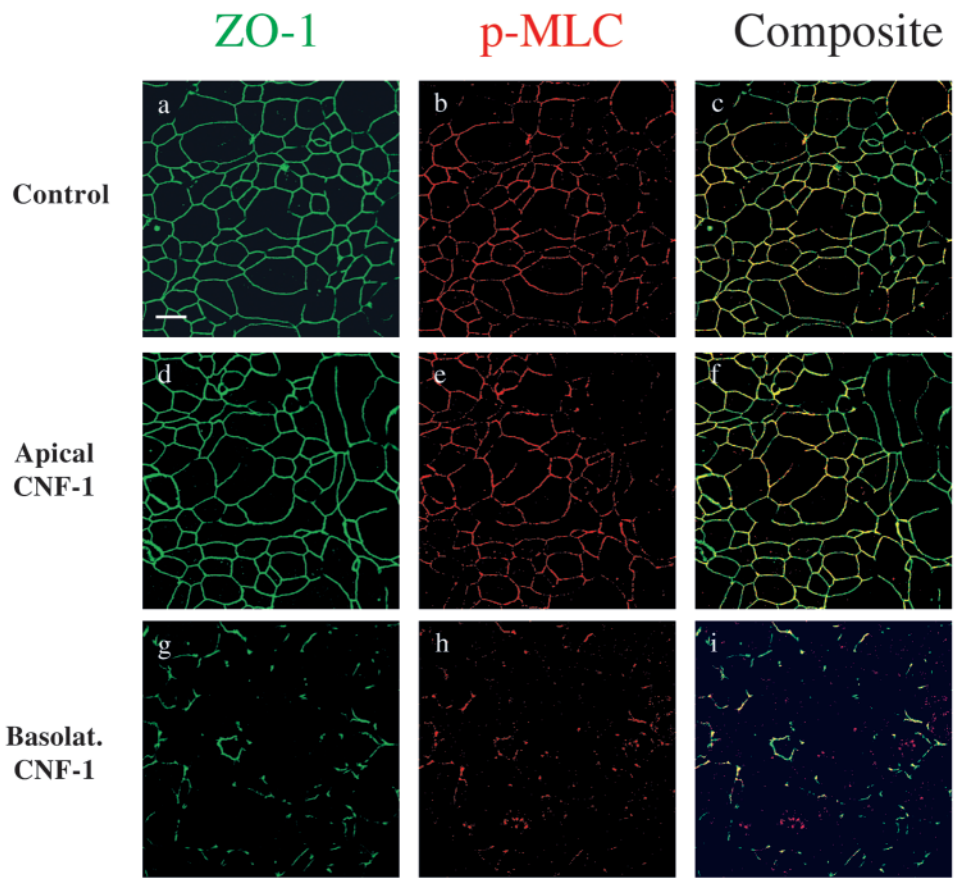

Fig. 7. CNF-1 disrupts morphological localization of a TJ-associated pool of phosphorylated MLC. In control T84 monolayers double-labeled with antibodies to ZO-1 (a; green) and p-MLC (b; red), extensive co-localization (c; yellow) was observed in the TJ plane. In monolayers treated apically for 24 hours with CNF toxin, ZO-1 (d) and p-MLC (e) were also seen to co-localize (f). However, monolayers treated basolaterally with CNF-1 for the same time period displayed not only profound disruption of ZO-1 staining (g) but also p-MLC (h) in the TJ plane. Fragments of each protein from the disassembled ring structures co-localized in a punctate pattern (i). Bar≈10 μm.

A more straightforward approach towards understanding the contributions of individual Rho GTPases to epithelial barrier function involves the over-expression of constitutively active/dominant-negative mutants of each GTPase. Stable expression of dominant-active Rho reportedly increases renal epithelial TER (Hasegawa et al., 1999). It is possible that dominant-active Rho 'swamps' a cell with signaling GTPase, potentially engaging effectors not normally activated physiologically, and thereby eliciting unusual TER phenomena. Additionally, in low-resistance monolayers such as those used in the study in question (Hasegawa et al., 1999), TER is a less-sensitive index of barrier function than the assessment of paracellular flux. Since paracellular permeability increased during dominant-active Rho expression (Hasegawa et al., 1999), this corroborates our results indicating compromised epithelial barrier function during Rho GTPase activation. Inducible expression systems that allow precise manipulation of mutant expression levels are a further improvement on stable expression systems where the mutant transgene is continuously 'on'. Using an elegant system, convincing evidence for an involvement of RhoA in disruption of epithelial barrier function has been obtained with tetracycline-repressible dominant-active Rho transfected into MDCK cells (Jou et al., 1998). In this system, dominant-active Rho mutant induction correlated with inability to form high TER (Jou et al., 1998). Thus, data by Jou et al., 1998 complements our use of CNF-1 to manipulate pharmacologically the activity of Rho GTPases (Jou et al., 1998). Additionally, our study attempted to characterize further the likely reasons for the disturbance of epithelial barrier

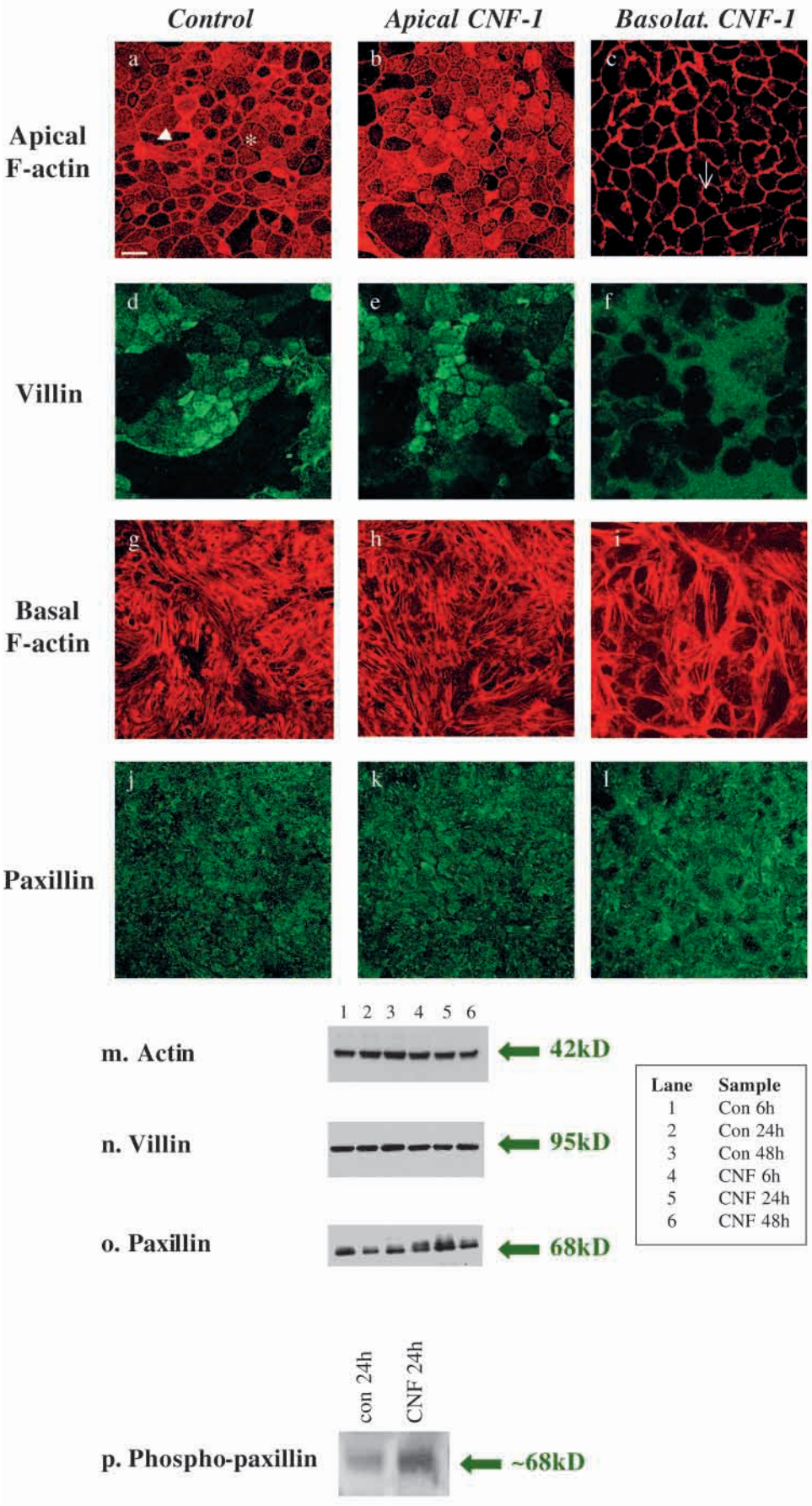

Fig. 8. CNF-1 induces polarized restructuring of F-actin and actin-binding proteins in epithelial monolayers. Rhodamine phalloidin was used to highlight F-actin organization in the apical and basal poles of T84 epithelial cells following polarized incubation with CNF-1 or vehicle control. While control monolayers (a) and those incubated apically with CNF-1 (b) revealed identical organization of F-actin in en face confocal micrographs, basolateral exposure to CNF-1 (c) induced dramatic polarized F-actin restructuring. Slight increases in staining intensity were observed in the perijunctional F-actin ring, but the normal pattern of punctate microvillous staining was virtually abolished in the apical pole of these monolayers (arrow) relative to controls. These changes were accompanied by altered immunolocalization of the brush border actin-binding protein villin in CNF-treated monolayers (f) relative to control cells (d) and those treated apically with toxin (e). F-actin distribution at the basal epithelial pole was similar in both control (g) and apically-treated monolayers (h), and consisted of diffuse meshworks of short stress fibers. By contrast, basolateral exposure to CNF-1 (i) stimulated the aggregation of stress fibers into thicker, 'cabled' bundles. Parallel changes were detected in immunolocalization of the actin-binding protein paxillin at the basal epithelial pole. Control monolayers (j) displayed 'plaque-like' paxillin immunoreactivity, similar to that in monolayers exposed apically to toxin (k). Basolateral treatment with CNF-1 (l) was associated with a slight increase in plaque number and size. CNF-induced changes in F-actin, villin and paxillin (m, n, o, respectively) were not accounted for by changes in the total levels of these proteins as assessed by western blot analysis of lysates from control (lanes 1-3) and CNF-treated monolayers (lanes 4-6) for the times indicated. Slight increases in the molecular mass of paxillin upon CNF incubation reflected tyrosine phosphorylation of the protein, as shown by the increased level of phospho-specific paxillin detected in lysates from CNF-treated cells relative to controls (p). Bar≈10 μm.

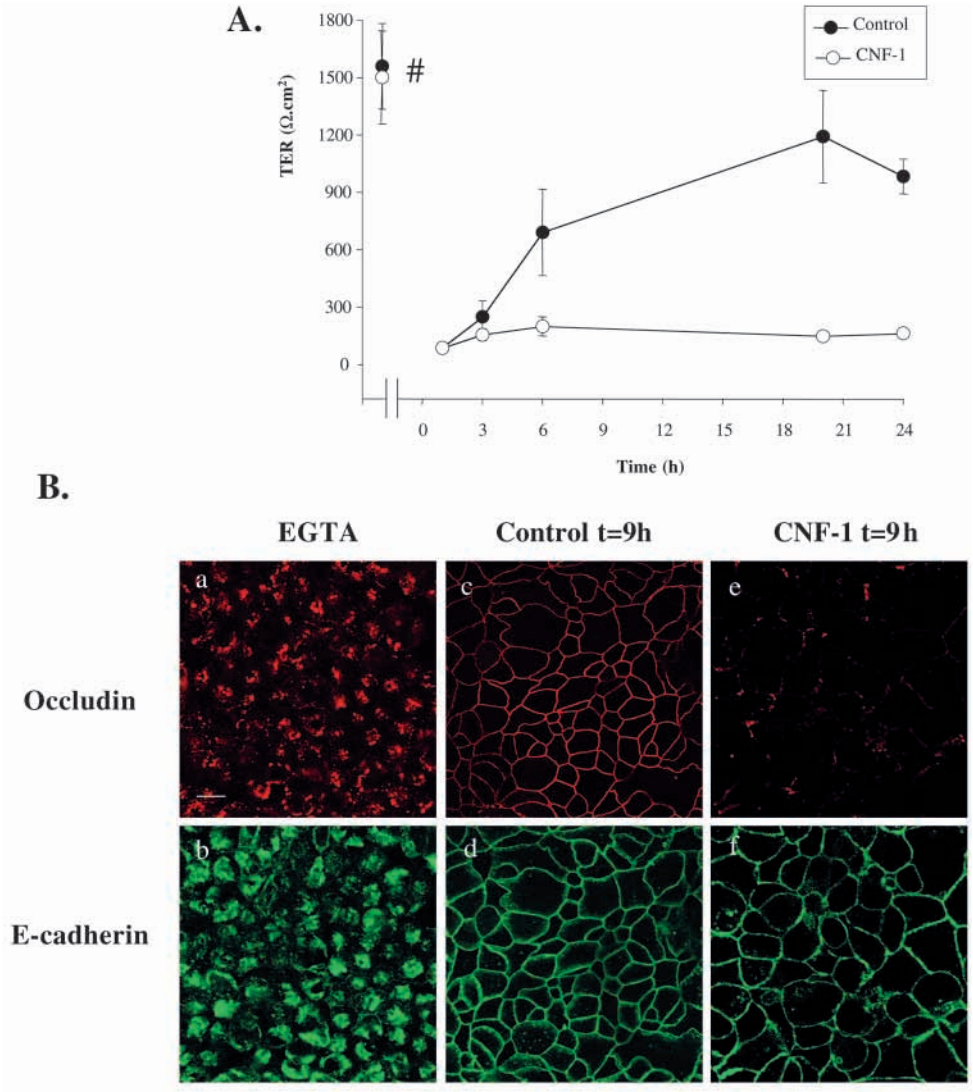

Fig. 9. CNF-1 impairs the assembly of junctions in calcium switch assays. (A) T84 monolayers exposed to EGTA (2 mM) in calcium- and magnesium-free media were allowed to recover in complete culture media (containing calcium and serum) in the presence of CNF-1 (1 nM) or vehicle. TER was monitored over time and used to assess the recovery of cell-cell contact. Monolayers exhibited high resistances prior to EGTA treatment (#), which dropped to ~10 Ω.cm^2 following EGTA incubation (not shown). During the recovery period, control monolayers recovered high TER values of >700 Ω.cm^2 after approximately 6 hours. By contrast, monolayers exposed to CNF-1 during recovery failed to reach TER values >170 Ω.cm^2 (n=4) by 24 hours, indicating impaired junctional reassembly. (B) Occludin and E-cadherin staining was examined in monolayers immediately after EGTA treatment, and following recovery for 9 hours in complete media containing either CNF-1 (1 nM) or vehicle. Following EGTA treatment, both proteins were seen to move away from the lateral membrane into an intracellular compartment (a,b). During recovery in complete media with vehicle, both occludin (c) and E-cadherin (d) redistributed correctly into characteristic ring structures at the lateral membrane. By contrast, monolayers exposed to CNF-1 appeared to assemble only E-cadherin but not occludin into ring structures at the same time period (e,f).

function, in the context of alterations in TJ proteins and F-actin organization.

Several lines of evidence suggest that CNF-induced perturbations of barrier function are non-cytotoxic (data not shown). First, TER values did not drop below ~300 Ω.cm^2, discounting frank cytotoxicity. Second, cell death was not observed in CNF-treated monolayers stained with hematoxylin/eosin. Finally, mitochondrial bioreduction of a tetrazolium salt was unimpaired in CNF-treated monolayers relative to control monolayers. Additionally, it has been reported that CNF-1 might in fact protect against apoptosis by enhancing cell-matrix adherence and cell spreading (Fiorentini et al., 1997; Fiorentini et al., 1998b), possibly related to enhanced F-actin stress fiber aggregation mediated by activated Rho (Ridley and Hall, 1992). There is also evidence that CNF-1 exerts an additional anti-apoptotic influence by increasing the expression of proteins in the Bcl-2 family (Fiorentini et al., 1998c).

To explore reasons for epithelial permeability defects induced upon activation of Rho GTPases, we began by examining the status of key proteins that localize in the TJ and exert regulatory control over the paracellular pathway. Significant redistribution of TJ proteins occludin, ZO-1 and JAM was observed following basolateral treatment with CNF-1. Similar effects were also observed for claudin-1 (data not shown). Occludin and ZO-1 immunolocalization in characteristic TJ ‘ring structures’ was severely disrupted, resulting in almost complete lack of continuity. JAM localization too was disturbed but, unlike occludin and ZO-1, did not virtually ‘disappear’ from the plane of the TJ membrane in response to basolateral treatment with CNF-1. Instead, broad, blurred rings of JAM were evident in en face confocal images, indicating some JAM redistribution below the TJ membrane in contrast to its former presence in a sharply localized ring at the TJ itself. It is intriguing to speculate why the disruption of JAM is not as drastic as that of occludin and ZO-1. This might relate to a necessity for JAM localization at the TJ membrane for correct assembly of the TJ protein complex (Liu et al., 2000), otherwise loss of this protein could prove detrimental for the capability of T84 monolayers to re-establish barrier function after transient insult by toxins such as CNF-1.

Our observations extend reports of irregular ZO-1 staining in MDCK cells transiently induced to express dominant-active

RhoA (Jou et al., 1998; Hasegawa et al., 1999). However, continuous expression of the same construct reportedly does not affect (Takaishi et al., 1997) or even enhances (Gopalakrishnan et al., 1998) ZO-1 localization at MDCK cell contact sites. The limitations of inducible versus continuous expression systems have been mentioned regarding inconsistencies between TER/permeability data. ZO-1 localization was reportedly unaffected in T84 cells exposed to CNF-1 for 10-16 hours (Hofman et al., 1998). However, control ZO-1 staining in this model was uncharacteristically diffuse, probably representing antibody specificity issues. Thus, nonspecific ZO-1 staining could obscure the detection of differences between control and CNF-treated monolayers. Our studies provide evidence that many proteins move away from the TJ upon overactivation of Rho GTPases, potentially explaining CNF-induced deficits in epithelial barrier function. We have also observed similar effects using an alternative intestinal epithelial model, the Caco-2 cell line, which is also a highly validated model for the study of TJs and barrier function.

In an attempt to explain why dramatic CNF-induced reductions in TJ protein immunostaining were not accompanied by biochemical loss of protein, we performed immunogold electron microscopy on T84 monolayers in order to define better the precise localization of TJ proteins following CNF-1 treatment. In control cells treated only with vehicle, occludin labeling was confined to areas of cell-cell contact, mainly in the uppermost 250 nm of the basolateral plasma membrane. Following exposure to CNF-1, some occludin remained at this site but a significant amount was internalized in endosomal/caveolar-like membranous structures, evidenced by co-localization of TJ proteins with caveolin-1 (also significantly internalized away from the TJ). Similar trends were observed for ZO-1 internalization and co-localization with caveolin-1 after CNF-1 treatment (data not shown). This is the first demonstration of TJ protein internalization in such structures following constitutive activation of Rho GTPases, and probably explains why profound reductions in TJ protein immunostaining were not accompanied by corresponding reductions in total TJ protein levels.

In order better to address the cellular destination of TJ proteins internalized following incubation with CNF-1, we double-stained monolayers for internalized occludin and a range of caveolar/endosomal markers. Strong co-localization was observed with the caveolar marker caveolin-1. A sub-pool of internalized occludin also co-localized with EEA-1-positive early endosomes and Rab11-positive recycling endosomes, but did not co-localize with late endosomes/lysosomes marked by LAMP-1. This provides novel evidence that TJ proteins can be internalized into endosomal compartments after toxin treatment. Dominant-active Rac1 and Cdc42 have been shown to affect endocytic trafficking in epithelial cells (Jou et al., 2000; Rojas et al., 2001), but little is known about the fate of TJ proteins following insult to the epithelium. Internalization of TJ proteins in caveolae or recycling endosomes is likely to have important functional consequences for cell survival. Proteins internalized in this process (sometimes termed potocytosis) appear to be protected from lysosomal degradation pathways unlike proteins internalized in classical clathrin-coated pits (Anderson, 1998; Mineo and Anderson, 2001). Thus, effective recycling of TJ proteins back to the membrane could occur in the absence of new protein synthesis, allowing faster re-establishment of barrier function. Since it is not clear exactly how much of each protein must remain at the TJ in order to maintain adequate barrier function, it must be speculated that any loss could adversely affect barrier properties to the extent observed in our functional assays following CNF-1 treatment. Interestingly, we have previously documented similar intracellular sequestration of TJ proteins following Rho protein inhibition with *C. difficile* toxins (Nusrat et al., 2001). Taken together, this illustrates that disruption of Rho GTPase function, whether excessive stimulation or indeed inhibition, adversely affects TJ structure and inevitably function.

Another important component of the TJ functional unit relates to its affiliations with cellular actin-myosin contractile machinery in the perijunctional F-actin ring. Inhibitors of MLC kinase have been shown to inhibit increases in paracellular permeability induced upon activation of the sodium-glucose transporter SGLT-1, which is physiologically important for enhancing nutrient uptake (Turner and Madara, 1995). Thus, the localization and phosphorylation status of MLC is likely to play an important role in governing paracellular permeability. In our study, basolateral treatment with CNF-1 significantly attenuated the presence of a pool of p-MLC co-localizing with ZO-1 at the TJ. However, CNF-induced enhancements in paracellular permeability could not be prevented using the MLC kinase inhibitor ML-7 (data not shown). This might reflect a two-way signaling mechanism, where CNF-1 mediates its effects by influencing TJ proteins that in turn modulate the underlying F-actin cytoskeleton. By contrast, certain physiological signals such as sodium-glucose co-transport act primarily by influencing F-actin/MLC, which also affects TJ function. Thus, phosphorylation of MLC could be more important as a physiological regulator of paracellular permeability (Turner and Madara, 1995) than as a pathophysiological target of bacterial toxins such as CNF-1. Additionally, since the presence of p-MLC at the TJ is crucial for contraction of the perijunctional F-actin ring, this could suggest that the primary permeability deficits induced by CNF-1 are not mediated by alterations in perijunctional ring contraction, but rather by another mechanism that might be related. This may prove an interesting area for further study, in the context of differences in the regulation of paracellular permeability between physiological stimuli such as glucose uptake and pathophysiological stimuli such as bacterial toxins.

In comparison to the profound effects of CNF-1 at the epithelial TJ, an interesting feature of our model is that the underlying adherens junction (AJ) was minimally disrupted. Some thickening or diffusion of E-cadherin and β-catenin was observed at cell-cell borders; however, the characteristic ‘ring structure’ patterns of both these proteins was largely preserved. Relative selectivity for TJs over AJs has also been observed upon direct inhibition of RhoA (Nusrat et al., 1995; Nusrat et al., 2001). Adhesive control at the AJ probably relates to Rac over Rho activity, since dominant-active Rac increased E-cadherin and β-catenin protein levels in MDCK cells (Takaishi et al., 1997). Therefore, the subtle alterations observed in AJ protein localization in our model might reflect Rac activation by CNF-1. However, CNF-induced morphological changes are most striking at the level of the TJ, a site where Rho exerts major structural and functional influence (Gopalakrishnan et

al., 1998; Hirase et al., 2001; Jou et al., 1998; Nusrat et al., 1995; Nusrat et al., 2001; Walsh et al., 2001). In light of the ability of CNF-1 to induce simultaneous activation of Rho, Rac and Cdc42, cross-talk between these three GTPases is likely to play a major role in the complex and intricate regulation of barrier function in epithelial cells.

Since the TJ has an intimate association with the F-actin cytoskeleton (Madara, 1987; Madara et al., 1987; Madara et al., 1988), we sought to explore further the role of Rho GTPase activation in regulating F-actin structures in polarized epithelial cells. Perijunctional F-actin was minimally affected in our system upon treatment with CNF-1, although slight increases in F-actin staining intensity at cell-cell borders were observed. This corroborates a report that CNF-1 stimulates F-actin accumulation at HEp-2 cell borders (Fiorentini et al., 1988) and might in fact reflect Rac rather than Rho activity, since dominant-active Rac stimulated F-actin accumulation at MDCK junctions (Takaishi et al., 1997). The most striking feature of basolateral exposure to CNF-1 was the almost complete loss of apical (microvillous) F-actin and its binding protein villin. Thus, as suggested, CNF-1 might efface apical microvilli (Hofman et al., 1998), but also disrupt the continuity between adjacent F-actin pools in the microvilli, perijunctional ring and the terminal web that could potentially destabilize TJ complex 'scaffolding'. However, as discussed in the context of reduced p-MLC localization at the TJ following incubation with CNF-1, contraction-based events might be secondary to mislocalization of TJ proteins as a mechanism for disrupting barrier function.

An interesting feature of the effects of CNF-1 on our model was polarized restructuring of F-actin. Thus, while apical F-actin was diminished, we observed prominent F-actin cables at the level of basal stress fibers, with some reorganization of paxillin, a focal adhesion protein that links actin to the extracellular matrix (Turner, 2000). Increased stress fiber density has been reported upon exposure to CNF-1 (Gerhard et al., 1998; Hofman et al., 1998) or activated Rho (Hasegawa et al., 1999; Takaishi et al., 1997). This mimics Rho-stimulated stress fiber formation in mesenchymal cells (Ridley and Hall, 1992). Increased basal F-actin might protect against injury to both epithelial (Barth et al., 1999) and endothelial (Vouret-Craviari et al., 1999) monolayers. Our findings represent restructuring of F-actin cytoskeletal structures, since total cellular levels of actin, villin and paxillin did not change in control versus CNF-treated monolayers. However, increased levels of tyrosine-phosphorylated paxillin were detected in CNF-treated samples relative to controls. This complements existing data showing enhanced tyrosine phosphorylation of paxillin in hepatoma cells treated with lysophosphatidic acid (LPA) by a RhoA/Rho kinase pathway (Imamura et al., 2000). Inhibition of Rho kinase has also been shown to prevent increases in tyrosine phosphorylation of paxillin observed upon bombesin treatment of Swiss 3T3 cells (Sinnett-Smith et al., 2001). However, in our system, the tyrosine kinase inhibitor genistein did not reverse any of the functional effects of CNF-1 such as reductions in TER or induced rearrangements in TJ protein localization (data not shown). Thus, tyrosine phosphorylation of paxillin upon Rho activation probably reflects polarized regulatory control of the basal F-actin network at the cell-matrix interface.

Rho GTPase regulation of TJ/AJ assembly was also analyzed using calcium switch assays (Liu et al., 2000). CNF-1 severely impaired TER recovery after transient calcium depletion. Recovery was similarly impaired in a related system, MDCK cells exposed to the ligand for a G-protein-coupled receptor activating RhoA (Hasegawa et al., 1999). Conflicting evidence was obtained by the same group using dominant-active RhoA transfectants, suggesting utilization of additional Rho effectors or perhaps negative regulation after swamping cells with actively signaling GTPase. In our system, CNF-induced impairment of recovery following calcium switch related to a direct effect on nascent TJs rather than AJs. Thus, we observed re-assembly of E-cadherin into ring-structures at the level of the AJ, whereas movement of occludin back to the TJ membrane was severely impaired in CNF-treated cells. Taken together with evidence of severe perturbations in TJs of confluent cells with mature junctions, this further illustrates the selectivity of CNF-1 for the TJ over the AJ.

While CNF-1 constitutively activates all Rho family members (Rho, Rac and Cdc42) (Lerm et al., 1999b), stress fiber assembly observed in our cells is highly consistent with RhoA activation (Ridley and Hall, 1992). Permeability alterations seem compatible with enhanced RhoA activity as reported to date, based on pharmacological studies and dominant-active RhoA mutants. However, it is not possible from our study to estimate the relative contributions of each activated GTPase to the functional changes observed. The low levels of RhoA activation observed in our assays in response to CNF-1 treatment may be sufficient to alter barrier function, particularly if Rho is concentrated in a highly enriched microenvironment at the cell surface as has been described previously (Michaely et al., 1999). High levels of Rac or Cdc42 activation might also be important in altering barrier function or, alternatively, other complementary cellular processes not directly investigated here. Additionally, cooperation between all three GTPases cannot be discounted as a mechanism for CNF-induced alterations in barrier function, since Cdc42 activation in fibroblasts has been reported to initiate sequential activation of Rac and Rho (Nobes and Hall, 1995).

Examination of specific effectors involved in Rho GTPase regulation of permeability is outside the scope of this study. However, multiple targets are potentially involved (Aspenstrom, 1999). Recent evidence suggests a role for Rho kinase (p160ROCK), which regulates actin-myosin contractility through multiple effects on myosin and its regulatory enzymes (Amano et al., 1996; Fukata et al., 1998; Kimura et al., 1996). Inhibition of Rho-induced permeability enhancements in endothelial/epithelial cells was recently shown with both dominant-negative Rho and a Rho kinase inhibitor (Hirase et al., 2001). Recent evidence from our laboratory has also implicated Rho kinase in regulating epithelial barrier function (Walsh et al., 2001). However, the Rho kinase inhibitor Y-27632 did not block the effects of CNF-1 on TER or TJ protein immunolocalization in our model (data not shown). This does not rule out the possibility that Rho kinase is involved, but merely underlines the difficulties in interpreting data obtained with two compounds both of which decrease barrier function.

In conclusion, our studies have demonstrated compromised intestinal epithelial barrier function upon constitutive activation of Rho GTPases with *E. coli* CNF-1. We have presented novel evidence that barrier deficits are probably

accounted for by movement of occludin and ZO-1 away from the TJ into membranous structures resembling caveolae/endosomes. Internalized TJ proteins might cycle through caveolin-containing rafts, and early and recycling endosomes, but appear to evade a degradative pathway involving late endosomes/lysosomes. Reports of TJ protein internalization in epithelial cells treated with clostridial toxins to inhibit Rho activity (Nusrat et al., 2001) illustrate the complexity of Rho GTPase-mediated regulation of TJ structure/function. Epithelial cells in vivo probably exert careful control over levels of activity/quiescence of Rho GTPase family members in order to preserve barrier function. While the role of CNF-1 as a virulence factor is controversial, it is possible that, by decreasing epithelial barrier function, the toxin facilitates access of luminal bacteria and proven virulence factors (such as hemolysin) to the sub-epithelial compartment. This could account for clinical correlations between the detection of CNF-1 and other virulence factors in diverse diseases (Andreu et al., 1997; Blanco et al., 1995; Caprioli et al., 1987; Elliott et al., 1998; Yuri et al., 1998). Furthermore, our study clearly supports a role of Rho GTPases in not only the maintenance of established TJs and paracellular permeability, but also the assembly of intercellular associations and recovery of barrier function.

We thank Susan Voss, A'Drian Pineda, Denice Esterly, Jason Chen, Amy Chang and G. Thomas Brown for expert technical support, and are grateful to Gilles Flatau, INSERM (Nice, France) for supplying us with CNF-1 toxin. This work was supported by the Crohn's and Colitis Foundation of America (research fellowship award to A.M.H., research grant to A.N.), and NIH grants DK53202 and DK59888 (A.N.).

References

Aktories, K. (1997). Bacterial toxins that target Rho proteins. *J. Clin. Invest.* **99**, 827-829.

Amano, M., Ito, M., Kimura, K., Fukata, Y., Chihara, K., Nakano, T., Matsuura, Y. and Kaibuchi, K. (1996). Phosphorylation and activation of myosin by Rho-associated kinase (Rho-kinase). *J. Biol. Chem.* **271**, 20246-20249.

Anderson, R. G. (1998). The caveolae membrane system. *Annu Rev. Biochem.* **67**, 199-225.

Andreu, A., Stapleton, A. E., Fennell, C., Lockman, H. A., Xercavins, M., Fernandez, F. and Stamm, W. E. (1997). Urovirulence determinants in *Escherichia coli* strains causing prostatitis [published erratum appears in *J. Infect Dis.* 1997 Nov;176(5):1416]. *J. Infect. Dise.* **176**, 464-469.

Aspenstrom, P. (1999). Effectors for the Rho GTPases. *Curr. Opin. Cell Biol.* **11**, 95-102.

Barth, H., Olenik, C., Sehr, P., Schmidt, G., Aktories, K. and Meyer, D. K. (1999). Neosynthesis and activation of Rho by *Escherichia coli* cytotoxic necrotizing factor (CNF1) reverse cytopathic effects of ADP-ribosylated Rho. *J. Biol. Chem.* **274**, 27407-27414.

Ben-Ami, G., Ozeri, V., Hanski, E., Hofmann, F., Aktories, K., Hahn, K. M., Bokoch, G. M. and Rosenshine, I. (1998). Agents that inhibit Rho, Rac, and Cdc42 do not block formation of actin pedestals in HeLa cells infected with enteropathogenic *Escherichia coli*. *Infect. Immun.* **66**, 1755-1758.

Blanco, M., Blanco, J., Blanco, J. E., Alonso, M. P., Abalia, I., Rodriguez, E., Bilbao, J. R. and Umaran, A. (1995). [Virulence factors and 0 serogroups of *Escherichia col*i as a cause of community-acquired urinary infections]. *Enferm. Infecc. Microbiol. Clin.* **13**, 236-241 [Spanish].

Boquet, P. (1999). Bacterial toxins inhibiting or activating small GTP-binding proteins. *Ann. N. Y. Acad. Sci.* **886**, 83-90.

Boquet, P., Sansonetti, P. J. and Tran Van Nhieu, G. (1999). Rho GTP-binding proteins as targets for microbial pathogens. *Prog. Mol. Subcell. Biol.* **22**, 183-199.

Caprioli, A., Falbo, V., Roda, L. G., Ruggeri, F. M. and Zona, C. (1983). Partial purification and characterization of an *Escherichia coli* toxic factor that induces morphological cell alterations. *Infect. Immun.* **39**, 1300-1306.

Caprioli, A., Donelli, G., Falbo, V., Possenti, R., Roda, L. G., Roscetti, G. and Ruggeri, F. M. (1984). A cell division-active protein from *E. coli*. *Biochem. Biophys. Res. Commun.* **118**, 587-593.

Caprioli, A., Falbo, V., Ruggeri, F. M., Baldassarri, L., Bisicchia, R., Ippolito, G., Romoli, E. and Donelli, G. (1987). Cytotoxic necrotizing factor production by hemolytic strains of *Escherichia coli* causing extraintestinal infections. *J. Clin. Microbiol.* **25**, 146-149.

Casanova, J. E., Wang, X., Kumar, R., Bhartur, S. G., Navarre, J., Woodrum, J. E., Altschuler, Y., Ray, G. S. and Goldenring, J. R. (1999). Association of Rab25 and Rab11a with the apical recycling system of polarized Madin-Darby canine kidney cells. *Mol. Biol. Cell* **10**, 47-61.

Contamin, S., Galmiche, A., Doye, A., Flatau, G., Benmerah, A. and Boquet, P. (2000). The p21 Rho-activating toxin cytotoxic necrotizing factor 1 is endocytosed by a clathrin-independent mechanism and enters the cytosol by an acidic-dependent membrane translocation step. *Mol. Biol. Cell* **11**, 1775-1187.

De Rycke, J., Nougayrede, J. P., Oswald, E. and Mazars, P. (1997). Interaction of *Escherichia coli* producing cytotoxic necrotizing factor with HeLa epithelial cells. *Adv. Exp. Med. Biol.* **412**, 363-366.

Denker, B. M. and Nigam, S. K. (1998). Molecular structure and assembly of the tight junction. *Am. J. Physiol.* **274**, F1-9.

Dharmsathaphorn, K. and Madara, J. L. (1990). Established intestinal cell lines as model systems for electrolyte transport studies. *Methods Enzymol.* **192**, 354-389.

Dharmsathaphorn, K., McRoberts, J. A., Mandel, K. G., Tisdale, L. D. and Masui, H. (1984). A human colonic tumor cell line that maintains vectorial electrolyte transport. *Am. J. Physiol.* **246**, G204-208.

Elliott, S. J., Srinivas, S., Albert, M. J., Alam, K., Robins-Browne, R. M., Gunzburg, S. T., Mee, B. J. and Chang, B. J. (1998). Characterization of the roles of hemolysin and other toxins in enteropathy caused by alpha-hemolytic *Escherichia coli* linked to human diarrhea. *Infect. Immun.* **66**, 2040-2051.

Falzano, L., Fiorentini, C., Donelli, G., Michel, E., Kocks, C., Cossart, P., Cabanie, L., Oswald, E. and Boquet, P. (1993). Induction of phagocytic behaviour in human epithelial cells by *Escherichia coli* cytotoxic necrotizing factor type 1. *Mol. Microbiol.* **9**, 1247-1254.

Fiorentini, C., Arancia, G., Caprioli, A., Falbo, V., Ruggeri, F. M. and Donelli, G. (1988). Cytoskeletal changes induced in HEp-2 cells by the cytotoxic necrotizing factor of *Escherichia coli*. *Toxicon* **26**, 1047-1056.

Fiorentini, C., Fabbri, A., Matarrese, P., Falzano, L., Boquet, P. and Malorni, W. (1997). Hinderance of apoptosis and phagocytic behaviour induced by *Escherichia coli* cytotoxic necrotizing factor 1: two related activities in epithelial cells. *Biochem. Biophys. Res. Commun.* **241**, 341-346.

Fiorentini, C., Gauthier, M., Donelli, G. and Boquet, P. (1998a). Bacterial toxins and the Rho GTP-binding protein: what microbes teach us about cell regulation. *Cell Death Differ.* **5**, 720-728.

Fiorentini, C., Matarrese, P., Straface, E., Falzano, L., Donelli, G., Boquet, P. and Malorni, W. (1998b). Rho-dependent cell spreading activated by *E. coli* cytotoxic necrotizing factor 1 hinders apoptosis in epithelial cells. *Cell Death Differ.* **5**, 921-929.

Fiorentini, C., Matarrese, P., Straface, E., Falzano, L., Fabbri, A., Donelli, G., Cossarizza, A., Boquet, P. and Malorni, W. (1998c). Toxin-induced activation of Rho GTP-binding protein increases Bcl-2 expression and influences mitochondrial homeostasis. *Exp. Cell Res.* **242**, 341-350.

Flatau, G., Lemichez, E., Gauthier, M., Chardin, P., Paris, S., Fiorentini, C. and Boquet, P. (1997). Toxin-induced activation of the G protein p21 Rho by deamidation of glutamine. *Nature* **387**, 729-733.

Fukata, Y., Kimura, K., Oshiro, N., Saya, H., Matsuura, Y. and Kaibuchi, K. (1998). Association of the myosin-binding subunit of myosin phosphatase and moesin: dual regulation of moesin phosphorylation by Rho-associated kinase and myosin phosphatase. *J. Cell Biol.* **141**, 409-418.

Gerhard, R., Schmidt, G., Hofmann, F. and Aktories, K. (1998). Activation of Rho GTPases by *Escherichia coli* cytotoxic necrotizing factor 1 increases intestinal permeability in Caco-2 cells. *Infect. Immun.* **66**, 5125-5131.

Gopalakrishnan, S., Raman, N., Atkinson, S. J. and Marrs, J. A. (1998). Rho GTPase signaling regulates tight junction assembly and protects tight junctions during ATP depletion. *Am. J. Physiol.* **275**, C798-809.

Gyles, C. L. (1992). *Escherichia coli* cytotoxins and enterotoxins. *Can. J. Microbiol.* **38**, 734-746.

Hall, A. (1998). Rho GTPases and the actin cytoskeleton. *Science* **279**, 509-514.

Hall, A. (1990). The cellular functions of small GTP-binding proteins. *Science* **249**, 635-640.

Hasegawa, H., Fujita, H., Katoh, H., Aoki, J., Nakamura, K., Ichikawa, A. and Negishi, M. (1999). Opposite regulation of transepithelial electrical resistance and paracellular permeability by Rho in Madin-Darby canine kidney cells. *J. Biol. Chem.* **274**, 20982-20988.

Hirase, T., Kawashima, S., Wong, E. Y., Ueyama, T., Rikitake, Y., Tsukita, S., Yokoyama, M. and Staddon, J. M. (2001). Regulation of tight junction permeability and occludin phosphorylation by RhoA-p160ROCK-dependent and -independent mechanisms. *J. Biol. Chem.* **276**, 10423-10431.

Hofman, P., Flatau, G., Selva, E., Gauthier, M., le Negrate, G., Fiorentini, C., Rossi, B. and Boquet, P. (1998). *Escherichia coli* cytotoxic necrotizing factor 1 effaces microvilli and decreases transmigration of polymorphonuclear leukocytes in intestinal T84 epithelial cell monolayers. *Infect. Immun.* **66**, 2494-2500.

Hopkins, A. M., Li, D., Mrsny, R. J., Walsh, S. V. and Nusrat, A. (2000). Modulation of tight junction function by G protein-coupled events. *Adv. Drug Deliv. Rev.* **41**, 329-340.

Imamura, F., Mukai, M., Ayaki, M. and Akedo, H. (2000). Y-27632, an inhibitor of rho-associated protein kinase, suppresses tumor cell invasion via regulation of focal adhesion and focal adhesion kinase. *Jpn J. Cancer Res.* **91**, 811-816.

Island, M. D., Cui, X., Foxman, B., Marrs, C. F., Stamm, W. E., Stapleton, A. E. and Warren, J. W. (1998). Cytotoxicity of hemolytic, cytotoxic necrotizing factor 1-positive and -negative *Escherichia coli* to human T24 bladder cells. *Infect. Immun.* **66**, 3384-3389.

Island, M. D., Cui, X. and Warren, J. W. (1999). Effect of *Escherichia coli* cytotoxic necrotizing factor 1 on repair of human bladder cell monolayers in vitro. *Infect. Immun.* **67**, 3657-3661.

Jou, T. S. and Nelson, W. J. (1998). Effects of regulated expression of mutant RhoA and Rac1 small GTPases on the development of epithelial (MDCK) cell polarity. *J. Cell Biol.* **142**, 85-100.

Jou, T. S., Schneeberger, E. E. and Nelson, W. J. (1998). Structural and functional regulation of tight junctions by RhoA and Rac1 small GTPases. *J. Cell Biol.* **142**, 101-115.

Jou, T. S., Leung, S. M., Fung, L. M., Ruiz, W. G., Nelson, W. J. and Apodaca, G. (2000). Selective alterations in biosynthetic and endocytic protein traffic in Madin-Darby canine kidney epithelial cells expressing mutants of the small GTPase Rac1. *Mol. Biol. Cell* **11**, 287-304.

Kazmierczak, B. I., Jou, T. S., Mostov, K. and Engel, J. N. (2001). Rho GTPase activity modulates *Pseudomonas aeruginosa* internalization by epithelial cells. *Cell. Microbiol.* **3**, 85-98.

Kimura, K., Ito, M., Amano, M., Chihara, K., Fukata, Y., Nakafuku, M., Yamamori, B., Feng, J., Nakano, T., Okawa, K. et al. (1996). Regulation of myosin phosphatase by Rho and Rho-associated kinase (Rho-kinase). *Science* **273**, 245-248.

Kranenburg, O., Poland, M., van Horck, F. P., Drechsel, D., Hall, A. and Moolenaar, W. H. (1999). Activation of RhoA by lysophosphatidic acid and Galpha12/13 subunits in neuronal cells: induction of neurite retraction. *Mol. Biol. Cell* **10**, 1851-1857.

Lemichez, E., Flatau, G., Bruzzone, M., Boquet, P. and Gauthier, M. (1997). Molecular localization of the *Escherichia coli* cytotoxic necrotizing factor CNF1 cell-binding and catalytic domains. *Mol. Microbiol.* **24**, 1061-1070.

Lerm, M., Schmidt, G., Goehring, U. M., Schirmer, J. and Aktories, K. (1999a). Identification of the region of rho involved in substrate recognition by *Escherichia coli* cytotoxic necrotizing factor 1 (CNF1). *J. Biol. Chem.* **274**, 28999-29004.

Lerm, M., Selzer, J., Hoffmeyer, A., Rapp, U. R., Aktories, K. and Schmidt, G. (1999b). Deamidation of Cdc42 and Rac by *Escherichia coli* cytotoxic necrotizing factor 1: activation of c-Jun N-terminal kinase in HeLa cells. *Infect. Immun.* **67**, 496-503.

Lerm, M., Schmidt, G. and Aktories, K. (2000). Bacterial protein toxins targeting Rho GTPases. *FEMS Microbiol. Lett.* **188**, 1-6.

Lesser, C. F., Scherer, C. A. and Miller, S. I. (2000). Rac, ruffle and rho: orchestration of *Salmonella* invasion. *Trends Microbiol.* **8**, 151-152.

Liu, Y., Nusrat, A., Schnell, F. J., Reaves, T. A., Walsh, S. V., Pochet, M. P. and Parkos, C. A. (2000). Human junction adhesion molecule regulates tight junction resealing in epithelia. *J. Cell Sci.* **113**, 2363-2374.

Mackay, D. J., Esch, F., Furthmayr, H. and Hall, A. (1997). Rho- and rac-dependent assembly of focal adhesion complexes and actin filaments in permeabilized fibroblasts: an essential role for ezrin/radixin/moesin proteins. *J. Cell Biol.* **138**, 927-938.

Madara, J. L. (1987). Intestinal absorptive cell tight junctions are linked to cytoskeleton. *Am. J. Physiol.* **253**, C171-175.

Madara, J. L. (1998). Regulation of the movement of solutes across tight junctions. *Ann. Rev. Physiol.* **60**, 143-159.

Madara, J. L. and Dharmsathaphorn, K. (1985). Occluding junction structure-function relationships in a cultured epithelial monolayer. *J. Cell Biol.* **101**, 2124-2133.

Madara, J. L., Moore, R. and Carlson, S. (1987). Alteration of intestinal tight junction structure and permeability by cytoskeletal contraction. *Am. J. Physiol.* **253**, C854-861.

Madara, J. L., Stafford, J., Barenberg, D. and Carlson, S. (1988). Functional coupling of tight junctions and microfilaments in T84 monolayers. *Am. J. Physiol.* **254**, G416-423.

Michaely, P. A., Mineo, C., Ying, Y. S. and Anderson, R. G. (1999). Polarized distribution of endogenous Rac1 and RhoA at the cell surface. *J. Biol. Chem.* **274**, 21430-21436.

Mineo, C. and Anderson, R. G. (2001). Potocytosis. Robert Feulgen Lecture. *Histochem. Cell Biol.* **116**, 109-118.

Nobes, C. D. and Hall, A. (1995). Rho, rac, and cdc42 GTPases regulate the assembly of multimolecular focal complexes associated with actin stress fibers, lamellipodia, and filopodia. *Cell* **81**, 53-62.

Nusrat, A., Giry, M., Turner, J. R., Colgan, S. P., Parkos, C. A., Carnes, D., Lemichez, E., Boquet, P. and Madara, J. L. (1995). Rho protein regulates tight junctions and perijunctional actin organization in polarized epithelia. *Proc. Natl. Acad. Sci. USA* **92**, 10629-10633.

Nusrat, A., Parkos, C. A., Verkade, P., Foley, C. S., Liang, T. W., Innis-Whitehouse, W., Eastburn, K. K. and Madara, J. L. (2000). Tight junctions are membrane microdomains. *J. Cell Sci.* **113**, 1771-1781.

Nusrat, A., von Eichel-Streiber, C., Turner, J. R., Verkade, P., Madara, J. L. and Parkos, C. A. (2001). *Clostridium difficile* toxins disrupt epithelial barrier function by altering membrane microdomain localization of tight junction proteins. *Infect. Immun.* **69**, 1329-1336.

Parkos, C. A., Colgan, S. P., Bacarra, A. E., Nusrat, A., Delp-Archer, C., Carlson, S., Su, D. H. and Madara, J. L. (1995). Intestinal epithelia (T84) possess basolateral ligands for CD11b/CD18-mediated neutrophil adherence. *Am. J. Physiol.* **268**, C472-479.

Ridley, A. J. and Hall, A. (1992). The small GTP-binding protein rho regulates the assembly of focal adhesions and actin stress fibers in response to growth factors. *Cell* **70**, 389-399.

Ridley, A. J., Paterson, H. F., Johnston, C. L., Diekmann, D. and Hall, A. (1992). The small GTP-binding protein rac regulates growth factor-induced membrane ruffling. *Cell* **70**, 401-410.

Rojas, R., Ruiz, W. G., Leung, S. M., Jou, T. S. and Apodaca, G. (2001). Cdc42-dependent modulation of tight junctions and membrane protein traffic in polarized Madin-Darby canine kidney cells. *Mol. Biol. Cell.* **12**, 2257-2274.

Sagi, S. A., Seasholtz, T. M., Kobiashvili, M., Wilson, B. A., Toksoz, D. and Brown, J. H. (2001). Physical and functional interactions of Galphaq with Rho and its exchange factors. *J. Biol. Chem.* **276**, 15445-15452.

Sanders, S. E., Madara, J. L., McGuirk, D. K., Gelman, D. S. and Colgan, S. P. (1995). Assessment of inflammatory events in epithelial permeability: a rapid screening method using fluorescein dextrans. *Epithelial Cell Biol.* **4**, 25-34.

Schmidt, G., Sehr, P., Wilm, M., Selzer, J., Mann, M. and Aktories, K. (1997). Gln 63 of Rho is deamidated by *Escherichia coli* cytotoxic necrotizing factor-1. *Nature* **387**, 725-729.

Schmidt, G. and Aktories, K. (1998). Bacterial cytotoxins target Rho GTPases. *Naturwissenschaften* **85**, 253-261.

Sears, C. L. and Kaper, J. B. (1996). Enteric bacterial toxins: mechanisms of action and linkage to intestinal secretion. *Microbiol. Rev.* **60**, 167-215.

Seasholtz, T. M., Zhang, T., Morissette, M. R., Howes, A. L., Yang, A. H. and Brown, J. H. (2001). Increased expression and activity of RhoA are associated with increased DNA synthesis and reduced p27(Kip1) expression in the vasculature of hypertensive rats. *Circ. Res.* **89**, 488-495.

Sinnett-Smith, J., Lunn, J. A., Leopoldt, D. and Rozengurt, E. (2001). Y-27632, an inhibitor of Rho-associated kinases, prevents tyrosine phosphorylation of focal adhesion kinase and paxillin induced by bombesin: dissociation from tyrosine phosphorylation of p130(CAS). *Exp. Cell Res.* **266**, 292-302.

Takaishi, K., Sasaki, T., Kotani, H., Nishioka, H. and Takai, Y. (1997). Regulation of cell-cell adhesion by Rac and Rho small G proteins in MDCK cells. *J. Cell Biol.* **139**, 1047-1059.

Troyanovsky, S. M. (1999). Mechanism of cell-cell adhesion complex assembly. *Curr. Opin. Cell Biol.* **5**, 561-566.

Turner, C. E. (2000). Paxillin interactions. *J. Cell Sci.* **113**, 4139-4140.

Turner, J. R. and Madara, J. L. (1995). Physiological regulation of intestinal epithelial tight junctions as a consequence of Na(+)-coupled nutrient transport. *Gastroenterology* **109**, 1391-1396.

Ullrich, O., Reinsch, S., Urbe, S., Zerial, M. and Parton, R. G. (1996). Rab11 regulates recycling through the pericentriolar recycling endosome. *J. Cell Biol.* **135**, 913-924.

von Eichel-Streiber, C., Boquet, P., Sauerborn, M. and Thelestam, M. (1996). Large clostridial cytotoxins – a family of glycosyltransferases modifying small GTP-binding proteins. *Trends Microbiol.* **4**, 375-382.

Vouret-Craviari, V., Grall, D., Flatau, G., Pouyssegur, J., Boquet, P. and Van Obberghen-Schilling, E. (1999). Effects of cytotoxic necrotizing factor 1 and lethal toxin on actin cytoskeleton and VE-cadherin localization in human endothelial cell monolayers. *Infect. Immun.* **67**, 3002-3008.

Walsh, S. V., Hopkins, A. M., Chen, J., Narumiya, S., Parkos, C. A. and Nusrat, A. (2001). Rho-kinase regulates tight junction function and is necessary for tight junction assembly in polarized intestinal epithelia. *Gastroenterology* **121**, 566-579.

Yuri, K., Nakata, K., Katae, H., Yamamoto, S. and Hasegawa, A. (1998). Distribution of uropathogenic virulence factors among *Escherichia coli* strains isolated from dogs and cats. *J. Vet. Med. Sci.* **60**, 287-290.